

Non-cytotoxic 1,2,3-triazole tethered fused heterocyclic ring derivatives display

Tax protein inhibition and impair HTLV-1 infected cells

Daiane Fernanda dos Santos^{a,b}, Denise Regina Bairros de Pilger^{c,d}, Charlotte Vandermeulen^e, Ricardo Khourif^f, Susimaire Pedersoli Mantoani^g, Paulo Sérgio Gonçalves Nunes^g, Peterson de Andrade^g, Ivone Carvalho^g, Jorge Casseb^h, Jean-Claude Twizere^e, Luc Willemsⁱ, Lucio Freitas-Junior^d & Simone Kashima^{a,b*}

^a*Ribeirão Preto Medical School, University of São Paulo, Ribeirão Preto, São Paulo, Brazil*

^b*Regional Blood Center of Ribeirão Preto, Ribeirão Preto, São Paulo, Brazil*

^c*Federal University of São Paulo, São Paulo, São Paulo, Brazil*

^d*Department of Microbiology, Biomedical Sciences Institute, University of São Paulo, São Paulo, São Paulo, Brazil*

^e*Protein Signaling and Interactions (GIGA), University of Liège, Liège, Belgium*

^f*Gonçalo Moniz Research Center (CPqGM), Oswaldo Cruz Foundation (FIOCRUZ), Salvador, Bahia, Brazil*

^g*School of Pharmaceutical Sciences of Ribeirão Preto, University of São Paulo, Ribeirão Preto, São Paulo, Brazil*

^h*Institute of Tropical Medicine of São Paulo, University of São Paulo, São Paulo, São Paulo, Brazil*

ⁱ*Molecular and Cellular Epigenetics (GIGA), University of Liège, Liège, Belgium*

*Corresponding author

E-mail address: daiane.fnd.santos@gmail.com (D. F. Santos)

Keywords: HTLV-1; ATL; compound screening; cell proliferation; apoptosis; Tax protein.

Abstract

Human T cell lymphotropic virus type 1 (HTLV-1) is a human retrovirus that infects approximately 10–20 million people worldwide and causes an aggressive neoplasia (adult T-cell leukemia/lymphoma - ATL). Therapeutic approaches for the treatment of ATL have variable effectiveness and poor prognosis, thus requiring strategies to identify novel compounds with activity on infected cells. In this sense, we initially screened a small series of 25 1,2,3-triazole derivatives to discover cell proliferation inhibitors and apoptosis inducers in HTLV-1-infected T-cell line (MT-2) for further assessment of their effect on viral *tax* activity through inducible-*tax* reporter cell line (Jurkat LTR-GFP). Eight promising compounds (**02**, **05**, **06**, **13**, **15**, **21**, **22** and **25**) with activity $\geq 70\%$ were initially selected, based on a suitable cell-based assay using resazurin reduction method, and evaluated towards cell cycle, apoptosis and Tax/GFP expression analyses through flow cytometry. Compound **02** induced S phase cell cycle arrest and compounds **05**, **06**, **22** and **25** promoted apoptosis. Remarkably, compounds **22** and **25** were also able to reduce GFP expression in an inducible-*tax* reporter cell, which suggests an effect on Tax viral protein. More importantly, compounds **02**, **22** and **25** were not cytotoxic in human hepatoma cell line (Huh-7). Therefore, the discovery of 3 active and non-cytotoxic compounds against HTLV-1-infected cells can potentially contribute, as an initial promising strategy, to the development process of new drugs against ATL.

Introduction

Human T-cell lymphotropic virus type 1 (HTLV-1) was the first human retrovirus discovered in 1980.¹⁻³ 10-20 million people are currently infected worldwide⁴ and some endemic areas, such as Japan, sub-Saharan Africa, the Caribbean region and South America, have been identified. In Brazil, for instance, serological studies in blood donors point out to 2.5 million infected habitants.⁵ Most HTLV-1-infected people remain asymptomatic, but after several decades, approximately 5% develop an aggressive neoplasia known as adult T-cell leukemia/lymphoma (ATL).^{6,7}

HTLV-1 infection is a real threat once there are no cure and preventive vaccine, as other neglected viral infections. Four clinical types of ATL, (acute, chronic, smoldering and lymphoma)⁸ are mainly treated with combination chemotherapy, which can culminate in the development of resistance or early relapse.^{9,10} A therapy using both interferon-alpha (IFN- α) and azidothymidine (AZT), a reverse transcriptase inhibitor, has been reported to be effective in smoldering or chronic clinical subtypes.^{11,12} Intense chemotherapy can be also followed by allogeneic hematopoietic stem cell transplantation.⁹ Recently, an anti-CCR4 monoclonal antibody (mogamulizumab) has been evaluated for the treatment of relapsed CCR4-positive ATL.¹³ Although acceptable tolerability of this antibody in patients, the risk of serious or fatal adverse effects must be considered.¹⁴

Efforts to develop new drugs to tackle ATL have been focused on HTLV-1 viral parts, such as the envelope glycoproteins, replication enzymes, reverse transcriptase, protease and integrase,¹⁵ besides the specific regulatory proteins Tax and HBZ (HTLV-1 bZIP factor). In particular, Tax viral protein has become an attractive target to treat ATL leukemogenesis due to its key role in the viral replication and oncogenic T-cell transformation.¹⁶ The Tax mode of action comprises transactivation of the HTLV-1

promoter, activation of the NF- κ B pathway for gene transcription, along with interactions with several host cell proteins involved in cell cycle, p53 dependent apoptosis and DNA repair.^{17,18} Tax protein is also responsible for up-regulation of the anti-apoptotic factor Bcl-2 and suppression of the pro-apoptotic factors Bim and Bid.¹⁹ Tax relevance in precluding apoptosis and promoting cell proliferation of infected cells certainly opens up possibility of therapeutic intervention upon its inhibition.²⁰ No promising Tax inhibitor has been reported to date, nevertheless the synthetic retinoid ST1926 promoted down regulation of the oncoprotein Tax, up regulation of p53 protein and induced cell cycle arrest as well as apoptosis in HTLV-1-infected cell lines.^{21,22}

The lack of Tax inhibitors favors the screen of compound libraries in order to identify potential prototypes. Click Chemistry is a well-known synthetic strategy that generates 1,2,3-triazole motifs and has been exploited to produce chemical diversity and obtain antitumor²³, antimicrobial²⁴ and antiviral agents.²⁵ In this context, we aimed to identify cell proliferation inhibitors and inducers of apoptosis in a cell-based assay (HTLV-1-infected cell line MT-2) by assessing a series of 25 heterocyclic compounds bearing 1,2,3-triazole motif. Additionally, a reporter cell line (Jurkat LTR-GFP) with inducible-*tax* expression was used to evaluate the effect of these compounds on *tax* activity.

Results

Based on a “Click Chemistry” strategy, 1,2,3-triazole derivatives were promptly obtained and purified by flash chromatography. Briefly, from a set of in-house and commercially available azides and alkynes, a small series of 25 compounds was synthesized via Copper-catalyzed Azide-Alkyne Cycloaddition reaction (CuAAC) in good yields and complete regioselectivity control since only 1,4-disubstituted 1,2,3-

triazoles were obtained.²⁶ Compounds bearing either aminoethyl-quinoline (compounds **01-08**), benzyl-piperazine (compounds **09-16**) or benzyl-piperidine (compounds **17-25**) scaffolds were linked through the triazole ring to generate a diverse range of aryl and heteroaryl compounds (indanone, phthalimide, indole, naphthyl, quinazoline, benzimidazole and coumarine) (Figure 1).

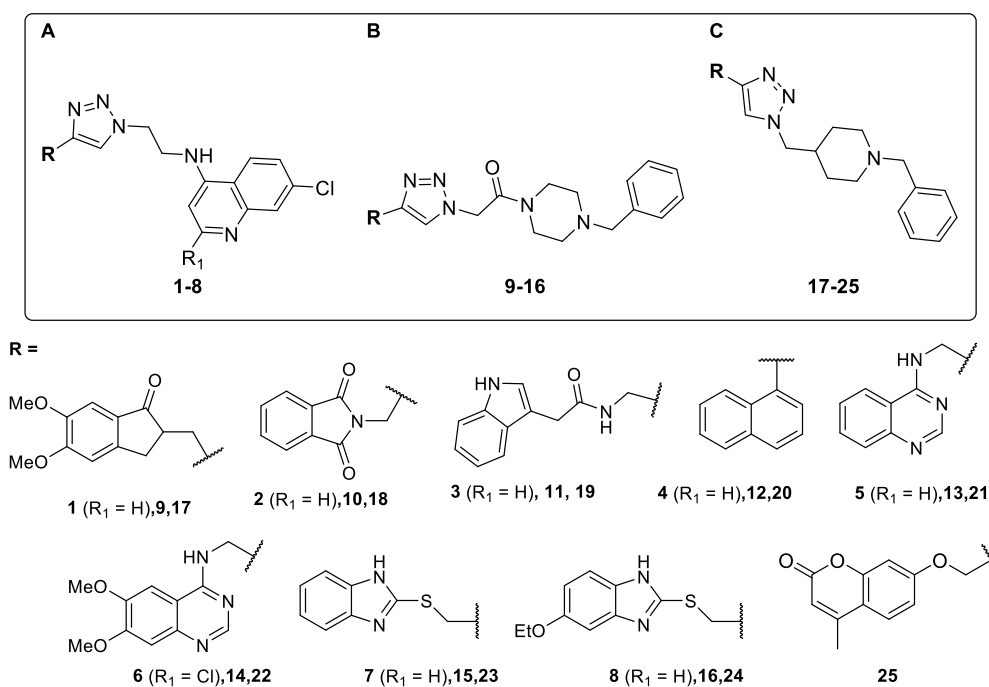


Figure 1. Series of synthetic compounds (**01 - 25**) for screening against HTLV-1-infected cell line (MT-2). Three sets of 1,2,3-triazole derivatives were chemically synthesized aiming at the specific scaffolds: A) aminoethyl-quinoline (compounds **01 - 08**); B) benzyl-piperazine (compounds **09 - 16**); C) benzyl-piperidine (compounds **17 - 25**).

The whole series of 1,2,3-triazole derivatives (50 μ M) was assessed towards the metabolic activity of HTLV-1-infected cell line (MT-2) using the resazurin reduction method as a simple, rapid and inexpensive way to evaluate cell proliferation and viability.²⁷ Most compounds were able to reduce the metabolic activity of MT-2 cell line, as well as the control ETO, in comparison to the negative control (MT-2 cell line with 0.5% DMSO) (Figure 2). Notably, eight compounds presented a greater effect on metabolic activity of MT-2: **02**, **05**, **06**, **13**, **15**, **21**, **22** and **25**, since they showed normalized inhibitory activity equal or superior to 70% (Figure 2).

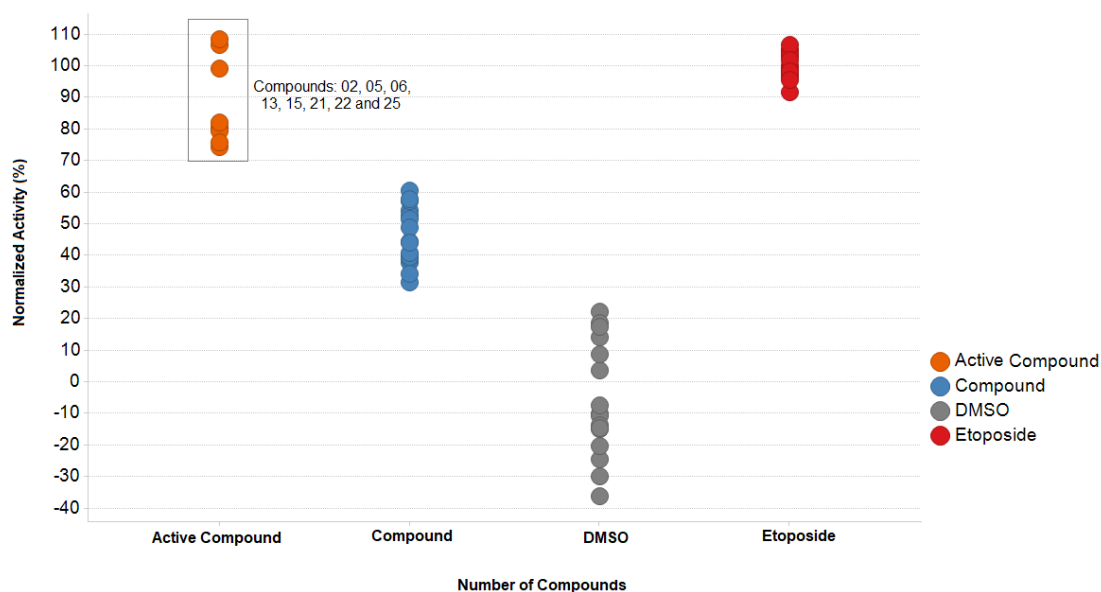


Figure 2. Metabolic activity of HTLV-1-infected cell line (MT-2) after incubation with different 1,2,3-triazole derivatives at 50 μM for 72 h. As controls: etoposide (ETO) at 20 μM and MT-2 cells with 0.5% DMSO (control). Before reaching 72 h, cells were incubated with resazurin for 4 h, whose fluorescence emitted was analysed by fluorometry at 590 nm. This graph is representative of one assay, in which axis *x* indicates the compounds and controls, and axis *y* indicates the percentage of normalized activity (inhibition of cell growth). Data normalization is referred to values of MT-2 with ETO. The most effective compounds (**02, 05, 06, 13, 15, 21, 22** and **25**) are exhibited in orange circles. The others compounds are shown in blue circles.

These eight promising compounds were further evaluated concerning the effect on MT-2 cell cycle. According to the results, only compound **02** induced an accumulation of cells at the S phase when compared to G0/G1 phase (Figure 3A) and the negative control DMSO (Figure 3B). Consequently, a lower percentage of MT-2 cells at the G2/M phase (Figure 3C) was observed and this effect on cell cycle was similar to the control ETO. The other compounds did not alter the cell proliferation significantly (Figure 3). Additionally, representative analyses of one experiment were included in the supporting information (Figure S1) showing histograms for each condition.

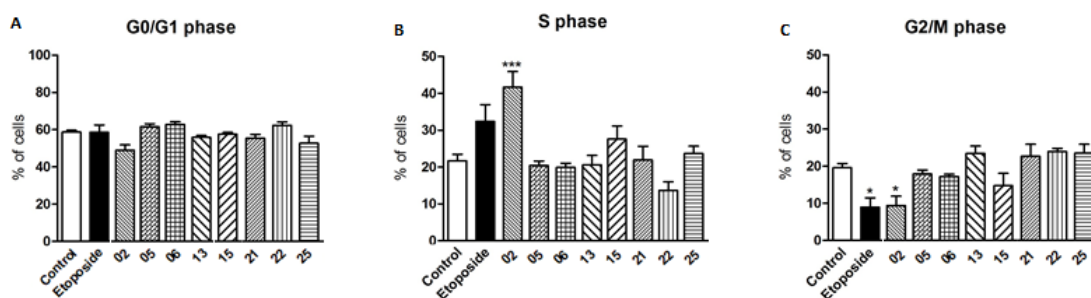


Figure 3. Effect of 1,2,3-triazole derivatives on cell cycle of HTLV-1-infected cell line (MT-2). Compounds at 50 μM were incubated with 3×10^5 cells (MT-2) for 72 h. As controls: etoposide (ETO) at 20 μM and MT-2 with 0.5% DMSO (control). After incubation time, cells were collected for cell cycle analysis by flow cytometry from staining with propidium iodide (PI). A total of 10,000 events was acquired and the graphs show the percentage of cells in G0/G1 (A), S (B) and G2/M (C) phases as mean \pm standard deviation. Statistical test: *One-way* ANOVA with post-test Tukey; * $p < 0.05$ and *** $p < 0.001$ compared to the control (MT-2 with 0.5% DMSO).

In order to examine the effects of the same eight promising compounds on apoptosis of MT-2 cells, the expression of active caspase-3/7 and annexin-V Cy5/PI was assessed by flow cytometry. We observed that compounds **05**, **06**, **22** and **25** induced apoptosis, since more positive cells for active caspase-3/7 were detected in relation to the negative control DMSO (Figure 4A). Likewise, staining for annexin-V/PI showed a greater percentage of apoptotic cells after culture in the presence of the same compounds (**05**, **06**, **22** and **25**) (Figure 4B). However, apoptosis induced by compound **25** was not statistically significant (mean \pm standard-deviation: $39.96 \pm 7.48\%$ vs. $18.70 \pm 5.33\%$, compound **25** and control DMSO, respectively; p value > 0.05). Representative analyses of one experiment for caspase-3/7 and annexin-V/PI staining were included in the supporting information (Figure S2 A and B, respectively).

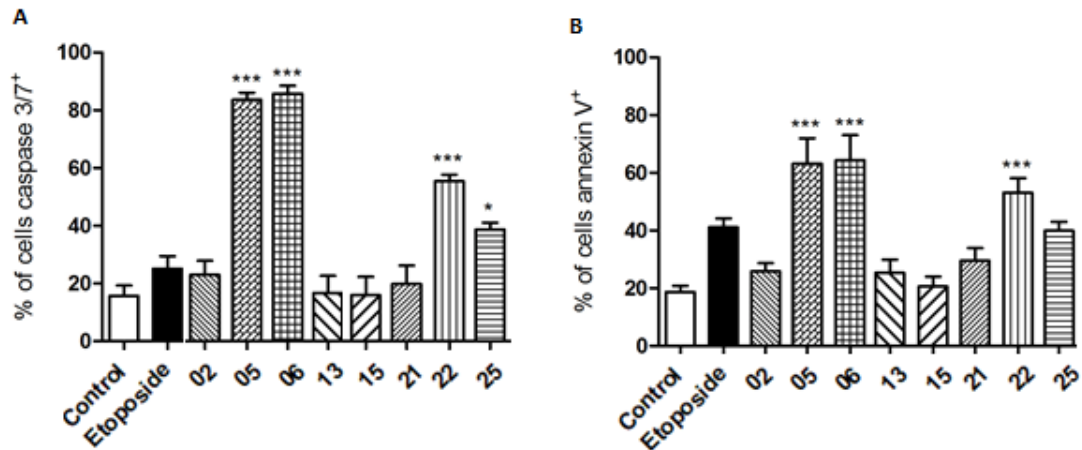


Figure 4. Compounds **05**, **06**, **22** and **25** promoted apoptosis of HTLV-1-infected cell line (MT-2). Compounds at 50 μ M were incubated with 3×10^5 cells for 72 h. As controls: etoposide (ETO) at 20 μ M and MT-2 with 0.5% DMSO (control). After that, cells were incubated with CellEvent™ Caspase-3/7 Green reagent during 45 minutes in order to evaluate the percentage of cells with active caspase-3/7 by flow cytometry (A). Then, apoptosis was also analyzed by annexin-V Cy5 and propidium iodide (PI) staining through flow cytometry, in which the percentage of cells annexin V⁺ indicates both initial and late apoptosis (B). The graphs exhibit the percentage of cells as mean \pm standard deviation. Statistical test: *One-way* ANOVA with post-test Tukey; * $p < 0.05$ and *** $p < 0.001$ in relation to control.

Furthermore, we performed the characterization of Jurkat LTR-GFP inducible-*tax* cell line to confirm the induction of *tax* gene expression under doxycycline stimulation (GFP expression). As expected, neither GFP expression in the absence of doxycycline (Figure 5A, I-II) nor significant GFP expression in Jurkat LTR-GFP Tet3G control cell line, after incubation with different concentrations of doxycycline, were observed as these cells did not have any gene of interest under the control of the TRE3G promoter (Figure S3). For Jurkat LTR-GFP inducible-*tax* cell line, a slight proportional increase of GFP expression based on the increase of doxycycline concentration was detected (Figure 5A). Thus, 1 μ g/mL was considered a suitable concentration of doxycycline for *tax* induction in this study. Moreover, Tax and GFP expressions were assessed by flow cytometry. It was confirmed that 43.1% of the viral protein expression (Tax) on Jurkat LTR-GFP inducible-*tax* was present in the cell population GFP⁺ (13.4%). HTLV-1-infected cell line

(MT-2) was used as positive control, which presented 65% expression of the viral Tax protein (Figure S4).

Based on Tax influence on cell growth and apoptosis during HTLV-1 infection, along with identification of those compounds that interfere on cell proliferation and apoptosis of MT-2 cell line, we further evaluated whether compounds **02**, **05**, **06**, **22** and **25** would present any potential inhibitory activity on LTR transactivation and/or *tax* gene expression. Therefore, we assessed the effect of these compounds on GFP expression of the Jurkat LTR-GFP inducible-*tax* cell line. Interestingly, compounds **22** and **25** reduced the percentage of viable cells expressing GFP when compared to the positive control with doxycycline (Jurkat LTR-GFP inducible-*tax* + doxycycline), Figure 5B-C. The decrease of GFP positive cells was similar to the control without doxycycline, whereas compound **02** did not alter the GFP expression. Although compounds **05** and **06** had also been able to decrease the percentage of viable cells expressing GFP (Figure 5B), a large number of dead cells GFP⁺PI⁺ was observed (compound **05**: $44.88 \pm 12.14\%$, and compound **06**: $90.98 \pm 1.36\%$, in comparison to control with doxycycline: $16.82 \pm 3.37\%$).

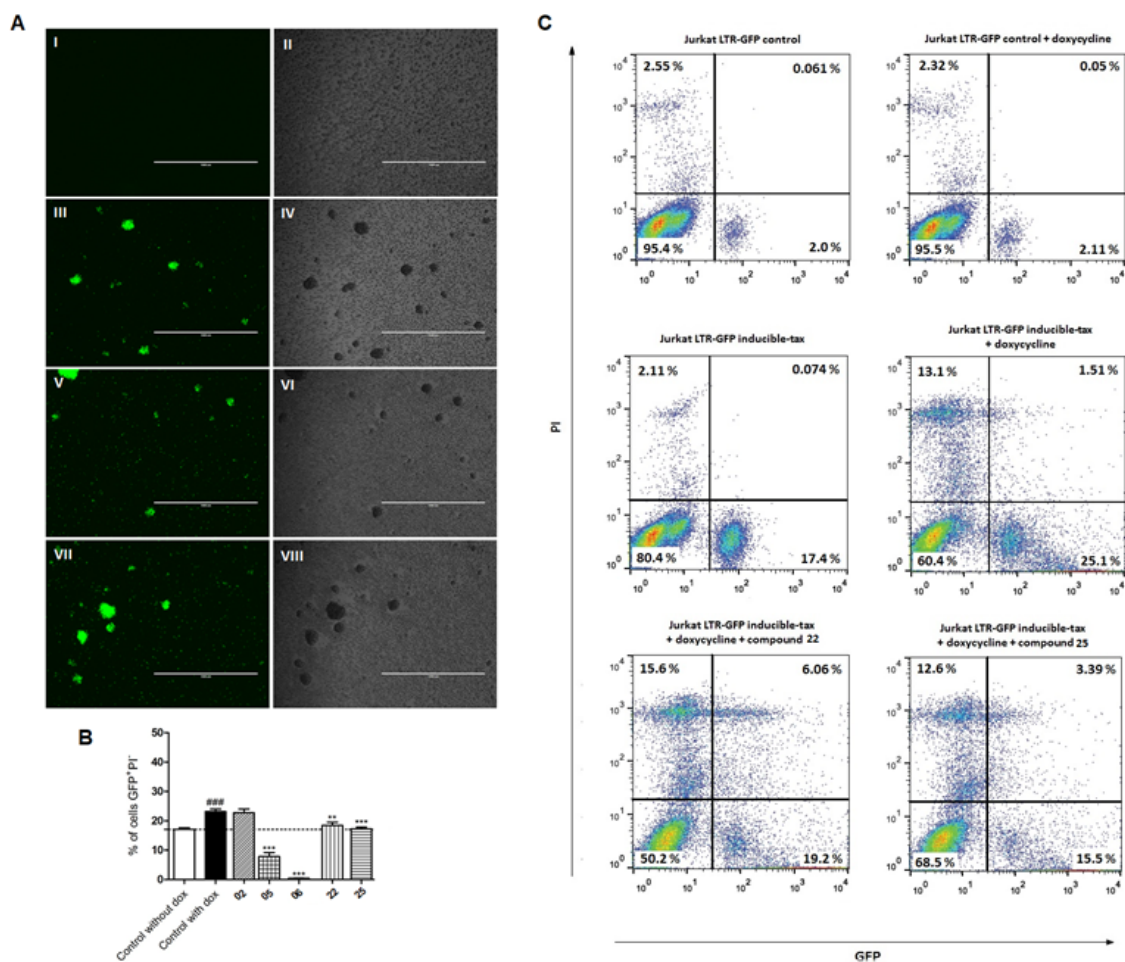


Figure 5. Effect of 1,2,3-triazole derivatives on GFP expression of Jurkat LTR-GFP inducible-*tax* cell line. A) Representative images of Jurkat LTR-GFP inducible-*tax* cell line: I-II) without doxycycline; III-IV) 0.01 $\mu\text{g}/\text{mL}$; V-VI) 0.1 $\mu\text{g}/\text{mL}$; VII-VIII) 1 $\mu\text{g}/\text{mL}$ (magnification: 4X, scale bar: 1,000 μm). B) Compounds at 50 μM were incubated with 3×10^5 cells for 72 h. As controls: Jurkat LTR-GFP inducible-*tax* with 0.5% DMSO (control without doxycycline, dox) and Jurkat LTR-GFP inducible-*tax* with 0.5% DMSO and doxycycline (control with dox). After that, cells were collected and PI was added to the samples. GFP expression into viable cells (PI-) was assessed through flow cytometry (BD FACSCalibur™). The graph shows the percentage of cells as mean \pm standard deviation. Statistical test: *One-way* ANOVA with post-test Tukey; ** $p < 0.01$ and *** $p < 0.001$ in relation to control with dox; ### $p < 0.001$ in relation to control without dox. C) Representative analyses using *FlowJo v10* software. A gate was performed according to size (forward scatter channel, FSC) and internal complexity (side scatter channel, SSC) of population, following by the determination of percentage of positive cells for GFP and PI through dot plot.

Based on the results with the human hepatoma cell line Huh-7, we observed that the active compounds **02**, **22** and **25** did not compromise the cellular viability in all concentrations tested (Figure 6 A-C). At the highest concentration (50 μM), viability

index of Huh-7 cell line was higher than 0.5 (mean \pm standard deviation: 0.85 ± 0.05 , compound **02**; 0.65 ± 0.09 , compound **22**; 0.61 ± 0.14 , compound **25**). On the other hand, compounds **05** and **06** drastically reduced the viability of Huh-7 cell line (mean \pm standard deviation: 0.0 ± 0.04 , compound **05**; 0.0 ± 0.03 , compound **06**) (Figure 6 D-E).

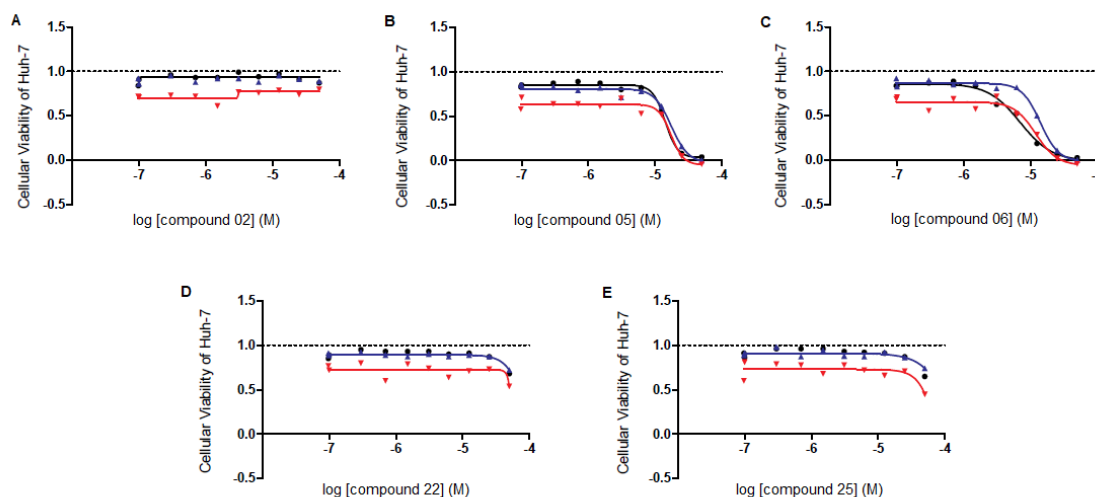


Figure 6. Cellular viability of human hepatoma cell line (Huh-7) after incubation with active compounds. During 72 h, Huh-7 cell line was cultured with compounds **02** (A), **05** (B), **06** (C), **22** (D) and **25** (E), which were diluted by a factor of 2. The cellular viability was analyzed by resazurin reduction method according to the equation described in item 2.9. Axis x indicates the concentration log of compound and axis y indicates the cellular viability. Each assay is represented by a colored curve.

Discussion

The emerging role of triazoles on antitumoral and antimicrobial activities^{23–26}, led us to exploit the 1,3-dipolar cycloaddition reaction (CuAAC: Copper-catalyzed Azide-Alkyne Cycloaddition reaction) to afford a small series of 25 1,2,3-triazole derivatives with chemical diversity based on three cores (Figure 1A-C), amino ethyl-quinoline (**01-08**), benzyl-piperazine (**09-16**) and benzyl-piperidine (**17-25**). We have synthesized this series in good yields and complete regioselectivity control and initially screened all compounds against HTLV-1-infected cells (MT-2 cell line), using resazurin reduction method, in order to identify cell proliferation inhibitors.

Resazurin reduction assay is well known and has been employed in some studies to screen compounds for ATL treatment due its reliability to test cell proliferation and/or viability and evaluate anti-proliferative effect on MT-1 and MT-2 cell lines.²⁷ For instance, a range of plant extracts have been tested by this method to isolate components with potent inhibitory activity for further tests,^{28,29} and YM155, an antitumor imidazolium compound and potent inhibitor of Survivin, was tested on a variety of human cancer cell lines, including T-acute lymphoblastic leukemia (T-ALL).³⁰

The initial screening on HTLV-1-infected cell line (MT-2) led us to select eight compounds (**02**, **05**, **06**, **13**, **15**, **21**, **22** and **25**) (Figure 2) for further studies as they significantly reduced the metabolic activity of the cells ($\geq 70\%$) in a similar manner to the positive control (ETO). In a follow-up experiment, we investigated whether the selected compounds could interfere in the cell cycle and induce apoptosis of MT-2 cell line. Remarkably, compound **02** was able to induce S phase cell cycle arrest (Figure 3), which is relevant considering that cell cycle relies on DNA replication and the subsequent cell division, besides being a process regulated by cyclins and cyclin-dependent kinases (CDKs).³¹ In fact, a selective CDK9 inhibitor (BAY 1143572) proved to have a strong potential to treat ATL³² and an interesting study has verified the activity of other compounds (BMS-345541 and purvalanol A) on cell cycle.³³

Taking into account the role of Tax protein in apoptosis inhibition of infected cells, we observed that half of the selected compounds (**05**, **06**, **22** and **25**) induced the activation of effector caspases-3/7 and the externalization of phosphatidylserine, thus contributing to apoptosis of MT-2 cell line (Figure 4).

Evidences that *tax* gene expression in HTLV-1-infected cells promotes up-regulation of anti-apoptotic and suppression of pro-apoptotic factors, and also *tax* expression is intermittent, since not all these cells express this viral gene during the

infection due to host immune surveillance evasion,³⁴ encouraged us to develop a suitable Jurkat LTR-GFP inducible-*tax* cell line to explore the mode of action of compounds **05**, **06**, **22** and **25**. From these cells, the induction of Tax expression by doxycycline was successfully accomplished in parallel with the consequent LTR transactivation for GFP expression (Figure 5A).

Therefore, we investigated whether the four selected compounds with action on cell proliferation and apoptosis of HTLV-1-infected cell line could also interfere in *tax* activity. Interestingly, compounds **22** and **25** clearly reduced GFP expression based on the inducible-*tax* reporter cell line results. Compounds **05** and **06** also decreased the percentage of GFP⁺ cells, but this activity was due to the higher number of dead cells in the analyses. Conversely, compound **02** did not reduce the GFP expression due to a possible interference in the regulators of cell cycle, such as cyclins and CDKs. However, the exact mechanism remains unclear. Overall, only compounds **22** and **25**, which were inducers of apoptosis in HTLV-1-infected cells, should be investigated as viral *tax* transactivation inhibitors. Furthermore, in contrast to compounds **05** and **06**, compounds **02**, **22** and **25** were not cytotoxic to the human hepatoma cell line Huh-7 uninfected by HTLV-1.

Conclusion

Taken together, the screening of a small series of 25 1,2,3-triazole derivatives provided eight promising compounds (**02**, **05**, **06**, **13**, **15**, **21**, **22** and **25**) capable of decreasing the metabolic activity of HTLV-1-infected cell line (MT-2) according to resazurin reduction method. Notably, compound **02** was able to interfere in the proliferation through induction of S phase cell cycle arrest. Regarding apoptosis, compounds **05**, **06**, **22** and **25** promoted significant activation of effector caspase-3/7

compared to the control. Similarly, these data were confirmed by annexin/PI staining. On the other hand, compounds **13**, **15** and **21** did not show significant activity on the cell cycle or apoptosis of HTLV-1-infected cell line (MT-2). We also proved that compounds **22** and **25**, besides causing apoptosis, have subtly inhibited GFP expression in the inducible-*tax* reporter cell line (Jurkat LTR-GFP), which suggests interference in LTR transactivation and/or *tax* expression. Therefore, the present study enabled the discovery of active and non-cytotoxic compounds (**02**, **22** and **25**) that can potentially contribute as an initial promising strategy to the challenging drug discovery campaign towards new therapeutics against ATL.

Acknowledgments

This study was supported by grants from Fundação de Amparo à Pesquisa do Estado de São Paulo (FAPESP, n. 2015/11566-0 and n. 2016/17301-1) and Conselho Nacional de Desenvolvimento Científico e Tecnológico (CNPq, n. 462290/2014-0). The authors thank Emmanuel Di Valentin, François Girouille and H  l  ne Gazon for the technical support in viral vectors production and cell transduction. We also thank Stephan Raafat and Camila de Oliveira Menezes for experimental support in flow cytometry; and Bruna Rodrigues Muys, Yuetsu Tanaka and Am  lcar Tanuri, for providing the cell cycle protocol, anti-Tax antibody (clone LT-4) and Huh-7 cell line, respectively.

References

1. Gallo, RC. History of the discoveries of the first human retroviruses: HTLV-1 and HTLV-2. *Oncogene*. 2005;24:5926–5930. <https://doi.org/10.1038/sj.onc.1208980>.
2. Poiesz, BJ, Ruscetti, FW, Gazdar, AF, et al. Detection and isolation of type C retrovirus particles from fresh and cultured lymphocytes of a patient with cutaneous T-

- cell lymphoma. *Proc Natl Acad Sci U S A*. 1980;77:7415–7419. <https://doi.org/10.1073/pnas.77.12.7415>.
3. Yoshida M. Discovery of HTLV-1, the first human retrovirus, its unique regulatory mechanisms, and insights into pathogenesis. *Oncogene*. 2005;24:5931–5937. <https://doi.org/10.1038/sj.onc.1208981>.
 4. Gessain A, Cassar O. Epidemiological aspects and world distribution of HTLV-1 infection. *Front Microbiol*. 2012;3:1–23. <https://doi.org/10.3389/fmicb.2012.00388>.
 5. Catalan-Soares B, Carneiro-Proietti ABF, Proietti FA. Heterogeneous geographic distribution of human T-cell lymphotropic viruses I and II (HTLV-I / II): Serological screening prevalence rates in blood donors from large urban areas in Brazil. *Cad Saúde Pública*. 2005;21:926–931. <https://doi.org/10.1590/S0102-311X2005000300027>.
 6. Bangham CR, Ratner L. How does HTLV-1 cause adult T-cell leukaemia/lymphoma (ATL)? *Curr Opin Virol*. 2015;14:93–100. <https://doi.org/10.1016/j.coviro.2015.09.004>.
 7. Ishitsuka K, Tamura K. Human T-cell leukaemia virus type i and adult T-cell leukaemia-lymphoma. *Lancet Oncol*. 2014;15:e517–e526. [https://doi.org/10.1016/S1470-2045\(14\)70202-5](https://doi.org/10.1016/S1470-2045(14)70202-5).
 8. Shimoyama M. Diagnostic criteria and classification of clinical subtypes of adult T-Cell leukaemia-lymphoma. *Br J Haematol*. 1991;79:428–437. <https://doi.org/10.1111/j.1365-2141.1991.tb08051.x>.
 9. Tsukasaki K, Tobinai K. Human T-cell lymphotropic virus type i-associated adult T-cell leukemia-lymphoma: New directions in clinical research. *Clin Cancer Res*. 2014;20:5217–5225. <https://doi.org/10.1158/1078-0432.CCR-14-0572>.

10. Marçais A, Suarez F, Sibon D, et al. Therapeutic options for adult T-cell leukemia/lymphoma. *Curr Oncol Rep.* 2013;15:457–464. <https://doi.org/10.1007/s11912-013-0332-6>.
11. Bazarbachi A, Plumelle Y, Ramos JC, et al. Meta-analysis on the use of zidovudine and interferon-alfa in adult T-cell leukemia/lymphoma showing improved survival in the leukemic subtypes. *J Clin Oncol.* 2010;28:4177–4183. <https://doi.org/10.1200/JCO.2010.28.0669>.
12. Kinpara S, Kijiyama M, Takamori A, et al. Interferon-A (IFN- α) suppresses HTLV-1 gene expression and cell cycling, while IFN- α combined with zidovudin induces p53 signaling and apoptosis in HTLV-1-infected cells. *Retrovirology.* 2013;10:1–15. <https://doi.org/10.1186/1742-4690-10-52>.
13. Ishida T, Joh T, Uike N, et al. Defucosylated anti-CCR4 monoclonal antibody (KW-0761) for relapsed adult T-cell leukemia-lymphoma: A multicenter phase II study. *J Clin Oncol.* 2012;30:837–842. <https://doi.org/10.1200/JCO.2011.37.3472>.
14. Ishitsuka K, Yurimoto S, Kawamura, et al. Safety and efficacy of mogamulizumab in patients with adult T-cell leukemia–lymphoma in Japan: Interim results of postmarketing all-case surveillance. *Int J Hematol.* 2017;106:522–532. <https://doi.org/10.1007/s12185-017-2270-9>.
15. Marino-Merlo F, Mastino A, Grelli S, et al. Future perspectives on drug targeting in adult T cell. *Front Microbiol.* 2018;9:1–8. <https://doi.org/10.3389/fmicb.2018.00925>.
16. Tanaka A, Matsuoka M. HTLV-1 alters T cells for viral persistence and transmission. *Front Microbiol.* 2018;9:1–7. <https://doi.org/10.3389/fmicb.2018.00461>.
17. Boxus M, Willems L. Mechanisms of HTLV-1 persistence and transformation. *Br J Cancer.* 2009;101:1497–1501. <https://doi.org/10.1038/sj.bjc.6605345>.

18. Carpentier A, Barez PY, Hamaidia M, et al. Modes of human T cell leukemia virus type 1 transmission, replication and persistence. *Viruses*. 2015;7:3603–3624. <https://doi.org/10.3390/v7072793>.
19. Mühleisen A, Giaisi M, Köhler R, et al. Tax contributes apoptosis resistance to HTLV-1-infected T cells via suppression of Bid and Bim expression. *Cell Death Dis*. 2014;5:1–10. <https://doi.org/10.1038/cddis.2014.536>.
20. Soltani A, Isaac S, Zahedi F, Soleimani A. Molecular targeting for treatment of human T-lymphotropic virus type 1 infection. *Biomed Pharmacother*. 2019;109:770–778. <https://doi.org/10.1016/j.biopha.2018.10.139>.
21. Hajj HE, Khalil B, Ghandour B, et al. Preclinical efficacy of the synthetic retinoid ST1926 for treating adult T-cell leukemia / lymphoma. *Blood*. 2014;124:2072–2081. <https://doi.org/10.1182/blood-2014-03-560060>.
22. Césaire R, Meniane JC. ST1926 repression of tax: ATL. *Blood*. 2014;124:2009–2012. <https://doi.org/10.1182/blood-2014-08-590489>.
23. Prachayasittikul V, Pingaew R, Anuwongcharoen N, et al. discovery of novel 1,2,3-triazole derivatives as anticancer agents using QSAR and in silico structural modification. *Springerplus*. 2015;4:1–22. <https://doi.org/10.1186/s40064-015-1352-5>.
24. Aziz Ali A, Gogoi D, Chaliha AK, et al. Synthesis and biological evaluation of novel 1,2,3-triazole derivatives as anti-tubercular agents. *Bioorganic Med Chem Lett*. 2017, 27, 3698–3703. <https://doi.org/10.1016/j.bmcl.2017.07.008>.
25. Kharb R, Shahar Yar M, Chander Sharma P. Recent advances and future perspectives of triazole analogs as promising antiviral agents. *Mini-Reviews Med Chem*. 2011;11:84–96. <https://doi.org/10.2174/138955711793564051>.

26. Mantoani SP, De Andrade P, Chierrito TPC, et al. Potential triazole-based molecules for the treatment of neglected diseases. *Curr Med Chem*. 2018;25:1–31. <https://doi.org/10.2174/0929867324666170727103901>.
27. Riss TL, Moravec RA, Niles AL, et al. Cell Viability Assays. *Assay Guid. Man*. 2013, 1–23.
28. Nakano D, Ishitsuka K, Hatsuse T, et al. Screening of promising chemotherapeutic candidates against human adult T-cell leukemia/lymphoma from plants: Active principles from *Physalis pruinosa* and structure-activity relationships with withanolides. *J Nat Med*. 2011;65:559–567. <https://doi.org/10.1007/s11418-011-0543-9>.
29. Nakano D, Ishitsuka K, Ikeda M, et al. Screening of promising chemotherapeutic candidates from plants against human adult T-cell leukemia/lymphoma (IV): Phenanthroindolizidine alkaloids from *Tylophora tanakae* leaves. *J Nat Med*. 2015;69:397–401. <https://doi.org/10.1007/s11418-015-0906-8>.
30. Sales L, De Souza GR, Ferreira-Silva G, et al. YM155 induces apoptosis in p53-deficient t-acute lymphoblastic leukemia cells independent of survivin inhibition. *Anticancer Drugs*. 2017;28:298–306. <https://doi.org/10.1097/CAD.0000000000000462>.
31. Otto T, Sicinski P. Cell cycle proteins as promising targets in cancer therapy. *Nat Rev Cancer*. 2017;17:93–115. <https://doi.org/10.1038/nrc.2016.138>.
32. Narita T, Ishida T, Ito A, et al. Cyclin-dependent kinase 9 is a novel specific molecular target in adult T-cell leukemia / lymphoma. *Blood*. 2017;130:1114–1125. <https://doi.org/10.1182/blood-2016-09-741983>.
33. Agbottah E, Yeh WI, Berro R, et al. Two specific drugs, BMS-345541 and purvalanol a induce apoptosis of HTLV-1 infected cells through inhibition of the NF-kappaB and cell cycle pathways. *AIDS Res Ther*. 2008;5:1–16. <https://doi.org/10.1186/1742-6405-5-12>.

34. Miyazato P, Matsuo M, Katsuya H, Satou Y. Transcriptional and epigenetic regulatory mechanisms affecting HTLV-1 provirus. *Viruses*. 2016;8:1–14. <https://doi.org/10.3390/v8060171>.

Supporting Information

Non-cytotoxic 1,2,3-triazole tethered fused heterocyclic ring derivatives display Tax protein inhibition and impair HTLV-1 infected cells

Daiane Fernanda dos Santos^{a,b}, Denise Regina Bairros de Pilger^{c,d}, Charlotte Vandermeulen^e, Ricardo Khourif^f, Susimaire Pedersoli Mantoani^g, Paulo Sérgio Gonçalves Nunes^g, Peterson de Andrade^g, Ivone Carvalho^g, Jorge Casseb^h, Jean-Claude Twizere^e, Luc Willemsⁱ, Lucio Freitas-Junior^d & Simone Kashima^{a,b*}

^aRibeirão Preto Medical School, University of São Paulo, Ribeirão Preto, São Paulo, Brazil

^bRegional Blood Center of Ribeirão Preto, Ribeirão Preto, São Paulo, Brazil

^cFederal University of São Paulo, São Paulo, São Paulo, Brazil

^dDepartment of Microbiology, Biomedical Sciences Institute, University of São Paulo, São Paulo, São Paulo, Brazil

^eProtein Signaling and Interactions (GIGA), University of Liège, Liège, Belgium

^fGonçalo Moniz Research Center (CPqGM), Oswaldo Cruz Foundation (FIOCRUZ), Salvador, Bahia, Brazil

^gSchool of Pharmaceutical Sciences of Ribeirão Preto, University of São Paulo, Ribeirão Preto, São Paulo, Brazil

^hInstitute of Tropical Medicine of São Paulo, University of São Paulo, São Paulo, São Paulo, Brazil

ⁱMolecular and Cellular Epigenetics (GIGA), University of Liège, Liège, Belgium

*Corresponding author

E-mail address: skashima@hemocentro.fmrp.usp.br (S. Kashima)

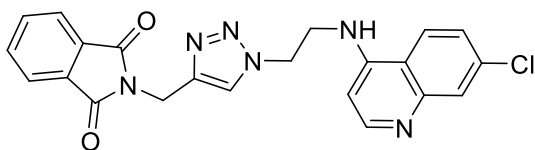
1. Materials and Methods

Synthesis

The whole series was obtained by employing the Copper-catalyzed Azide-Alkyne Cycloaddition (CuAAC) reaction as the final step to couple building blocks containing azide of quinolyl (compounds **1-8**), piperazinyl (compounds **9-16**) and piperidinyl (compounds **17-25**) moieties with the respective building blocks containing alkynes. The synthesis of compounds **17-25** is described by Andrade et al., 2018¹ and similarly employed to synthesize **1-16**.

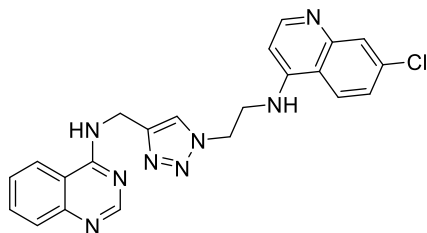
General Procedure for CuAAC reaction to obtain compounds **1-25** is described as follows: Catalytic amount of sodium ascorbate and CuSO₄ were added to a stirring solution of azido- and alkyne-building blocks in DCM/*t*-BuOH/H₂O or DMF. The reaction was stirred overnight at room temperature (compounds **17-25**) or irradiated on a microwave at 70 °C for 10 min (3 times, compounds **1-16**). After completion, toluene (2 x 10 mL) was added for solvents removal under vacuum. DCM (15 mL) was added to the crude and washed with H₂O (2 x 10 mL). The organic layer was dried over MgSO₄, filtered, concentrated and the crude was purified by flash chromatography to afford the desired compounds. Herein, we provide full analytical data for the promising compounds (**02**, **05**, **06**, **13**, **15** and **25**) selected from the cell-based assay using resazurin reduction method. The analytical data for compounds **21**, **22** (also selected in the screening) have already been published.¹

2-((1-(2-((7-chloroquinolin-4-yl)amino)ethyl)-1H-1,2,3-triazol-4-yl)methyl)isoindoline-1,3-dione (**02**)



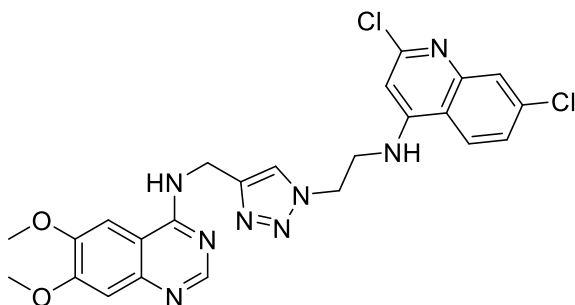
^1H NMR (400 MHz, CD_3OD) δ_{H} (ppm): 8.24 (1H, d, J 5.9 Hz), 7.96 (1H, d, J 9.1 Hz), 7.88 (1H, s), 7.84 – 7.78 (4H, m), 7.65 (1H, d, J 2.1 Hz), 7.38 (1H, dd, J 9.0, 2.1 Hz), 6.37 (1H, d, J 6.0 Hz), 4.76 – 4.66 (2H, m), 3.96 – 3.90 (2H, m), 1.96 (2H, s). ^{13}C NMR (101 MHz, CD_3OD) δ_{C} (ppm): 168.9, 150.7, 144.6, 135.5, 133.2, 126.8, 126.2, 125.7, 125.3, 124.3, 124.3, 99.3, 43.7, 33.6. HRMS (ES^+): m/z $[\text{M}+\text{H}]^+$ calculated for: $\text{C}_{22}\text{H}_{18}\text{ClN}_6\text{O}_2$: 433.1180; found: 433.1173.

N-((1-(2-((7-chloroquinolin-4-yl)amino)ethyl)-1H-1,2,3-triazol-4-yl)methyl)quinazolin-4-amine (**05**)



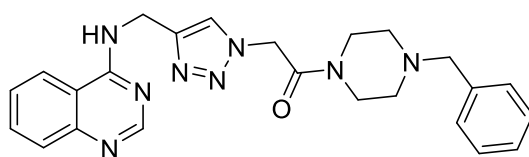
^1H NMR (300 MHz, $\text{DMSO-}d_6$) δ_{H} (ppm): 8.71 – 8.63 (1H, m), 8.32 (1H, s), 8.27 – 8.20 (1H, m), 8.08 (1H, d, J 8.0 Hz), 7.94 (2H, d, J 9.8 Hz), 7.71 – 7.52 (3H, m), 7.36 (2H, dd, J 13.4 Hz, J 6.0 Hz), 7.25 (1H, d, J 8.5 Hz), 6.39 (1H, d, J 4.6 Hz), 4.64 (2H, d, J 5.2 Hz), 4.48 (2H, t, J 5.3 Hz), 3.68 – 3.54 (2H, m). ^{13}C NMR (75 MHz, $\text{DMSO-}d_6$) δ_{C} (ppm): 159.2, 156.8, 155.0, 151.7, 149.9, 149.1, 144.9, 133.7, 132.7, 127.5, 127.3, 125.8, 124.5, 123.8, 123.8, 122.7, 47.7, 42.5, 39.5, 35.9. HRMS (ES^+): m/z $[\text{M}+\text{H}]^+$ calculated for $\text{C}_{22}\text{H}_{20}\text{ClN}_8$ 431.1499, found 431.1493.

N-((1-(2-((2,7-dichloroquinolin-4-yl)amino)ethyl)-1H-1,2,3-triazol-4-yl)methyl)-6,7-dimethoxyquinazolin-4-amine (**06**)



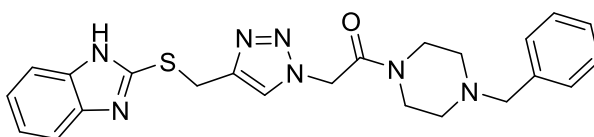
^1H NMR (300 MHz, $\text{DMSO-}d_6$) δ_{H} (ppm): 9.02 (1H, s), 8.50 (1H, s), 8.37 (1H, s), 8.07 – 7.97 (2H, m), 7.80 (1H, s), 7.65 (1H, s), 7.41 (1H, d, J 9.0 Hz), 7.13 (1H, s), 6.81 (1H, t, J 5.5 Hz), 4.76 (2H, d, J 4.6 Hz), 4.63 (2H, t, J 5.2 Hz), 4.15 – 4.12 (2H, m), 3.93 (3H, s), 3.88 (3H, s). ^{13}C NMR (75 MHz, $\text{DMSO-}d_6$) δ_{C} (ppm): 158.3, 154.6, 151.9, 148.9, 147.5, 146.31, 144.3, 141.9, 133.9, 127.7, 125.7, 124.5, 124.0, 119.7, 110.3, 107.9, 104.41, 102.3, 56.2, 56.0, 49.8, 45.6, 36.0. HRMS (ES^+): m/z $[\text{M}+\text{H}]^+$ calculated for $\text{C}_{24}\text{H}_{23}\text{Cl}_2\text{N}_8\text{O}_2$: 525.1321, found: 525.1311.

1-(4-benzylpiperazin-1-yl)-2-(4-((quinazolin-4-ylamino)methyl)-1H-1,2,3-triazol-1-yl)ethan-1-one (**13**)



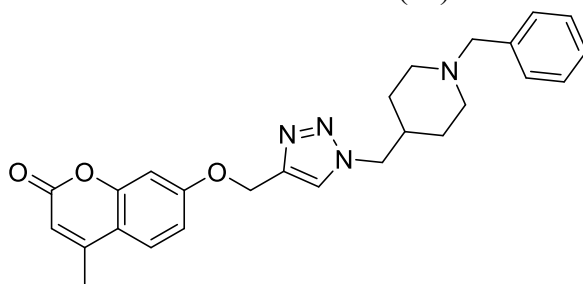
^1H NMR (300 MHz, CD_3OD) δ_{H} (ppm): 8.49 (1H, s), 8.10 (1H, d, J 8.2 Hz), 7.93 (1H, s), 7.85- 7.66 (2H, m), 7.51 (1H, t, J 7.5 Hz), 7.34- 7.17 (5H, m), 5.41 (2H, s), 4.90 (2H, s), 3.60 – 3.46 (6H, m), 2.46 (4H, dt, J 17.7 Hz, J 5.0 Hz). ^{13}C NMR (75 MHz, CD_3OD) δ_{C} (ppm): 166.2, 138.4, 134.4, 130.5, 129.4, 128.5, 127.6, 127.5, 123.5, 63.6, 53.7, 53.4, 52.0, 51.4, 49.8, 49.0, 45.9, 43.2, 37.3. HRMS (ES^+): m/z $[\text{M}+\text{H}]^+$ calculated for $\text{C}_{24}\text{H}_{27}\text{N}_8\text{O}$: 443.2308, found 443.2302.

2-(4-(((1H-benzo[d]imidazol-2-yl)thio)methyl)-1H-1,2,3-triazol-1-yl)-1-(4-benzylpiperazin-1-yl)ethan-1-one (**15**)



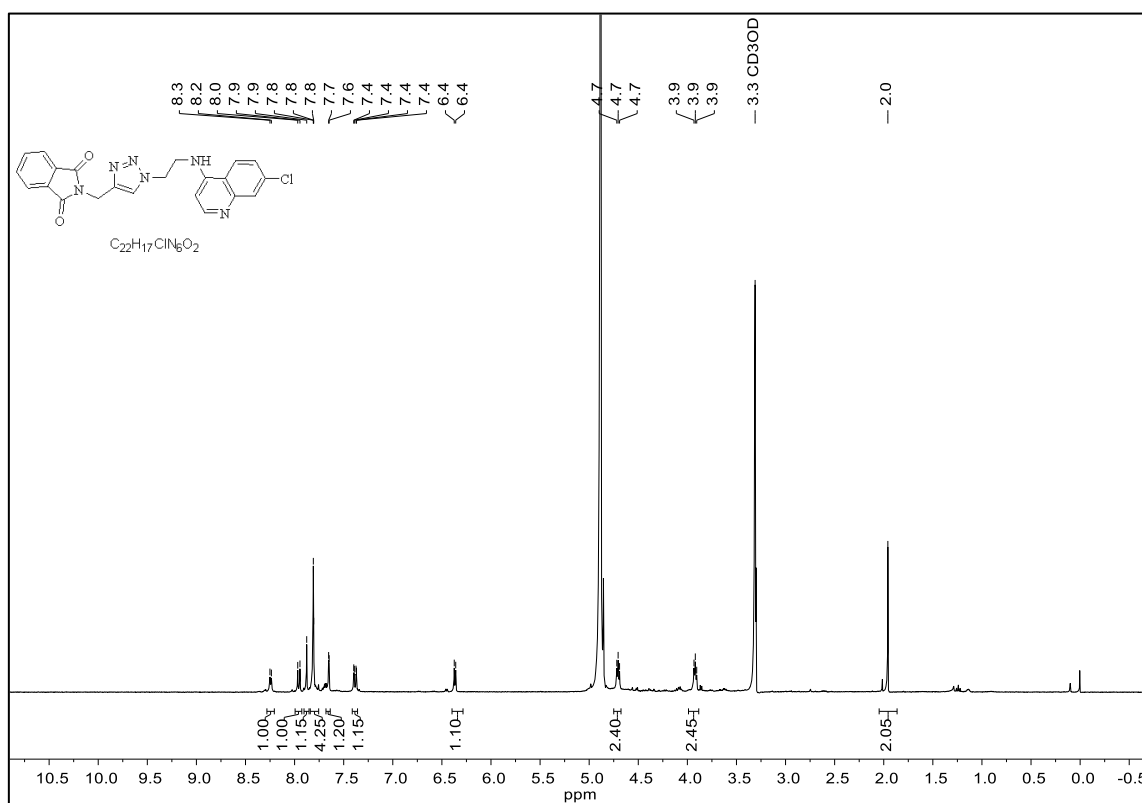
^1H NMR (300 MHz, CDCl_3) δ_{H} (ppm): 7.69 (1H, s), 7.54 (2H, dd, J 5.1, 2.5 Hz), 7.38 – 7.26 (5H, m), 7.20 (2H, dd, J 6.0, 3.2 Hz), 5.19 (2H, s), 4.41 (2H, s), 3.67 – 3.59 (2H, m), 3.51 (4H, d, J 4.8 Hz), 2.46 (4H, q, J 4.5 Hz). ^{13}C NMR (75 MHz, CDCl_3) δ_{C} (ppm): 163.2, 149.4, 145.5, 137.3, 129.2, 128.6, 127.6, 124.3, 122.5, 62.8, 52.8, 52.5, 51.2, 50.3, 45.4, 42.6, 27.2. HRMS (ES^+): m/z $[\text{M}+\text{H}]^+$ calculated for $\text{C}_{23}\text{H}_{26}\text{N}_7\text{OS}$: 448.1920; found: 448.1915.

7-((1-((1-benzylpiperidin-4-yl)methyl)-1H-1,2,3-triazol-4-yl)methoxy)-3,8a-dihydro-2H-chromen-2-one (**25**)

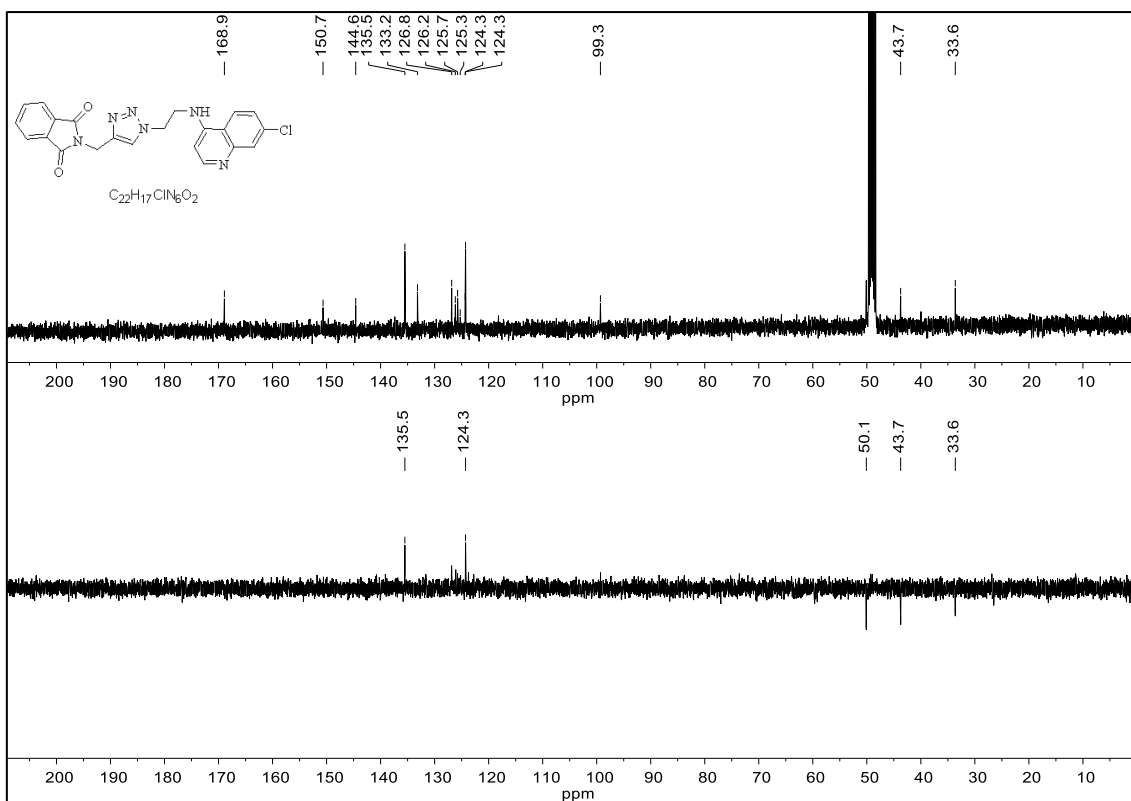


^1H NMR (300 MHz, CDCl_3) δ_{H} (ppm): 7.62 (1H, s), 7.51 (1H, d, J 8.7 Hz), 7.28 (6H, m), 6.94 (2H, m), 6.14 (1H, s), 5.25 (2H, s), 4.25 (2H, d, J 7.1 Hz), 3.51 (2H, s), 2.91 (2H, d, J 11.4 Hz), 2.39 (3H, s), 1.95 (3H, d, J 9.9 Hz), 1.67 – 1.18 (4H, m). ^{13}C NMR (75 MHz, CDCl_3) δ_{C} (ppm): 161.3, 161.2, 155.2, 152.6, 142.9, 129.3, 128.4, 127.3, 125.8, 123.6, 114.1, 112.5, 112.4, 102.2, 63.2, 62.4, 56.02, 52.92, 37.0, 29.7, 18.8. HRMS (ES^+): m/z $[\text{M}+\text{H}]^+$ calculated for $\text{C}_{26}\text{H}_{29}\text{N}_4\text{O}_3$: 445.2240; found: 445.2235.

^1H NMR (400 MHz, CD_3OD) – Compound **02**



¹³C NMR (101 MHz, CD₃OD) – Compound 02



HRMS (ES⁺) – Compound 02

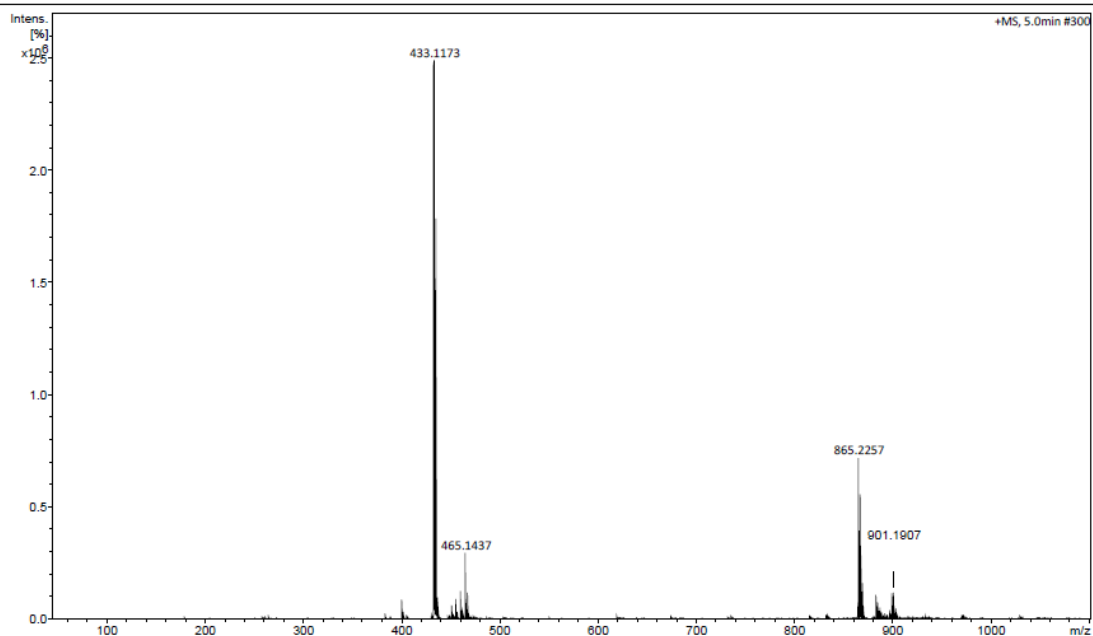
Generic Display Report

Analysis Info

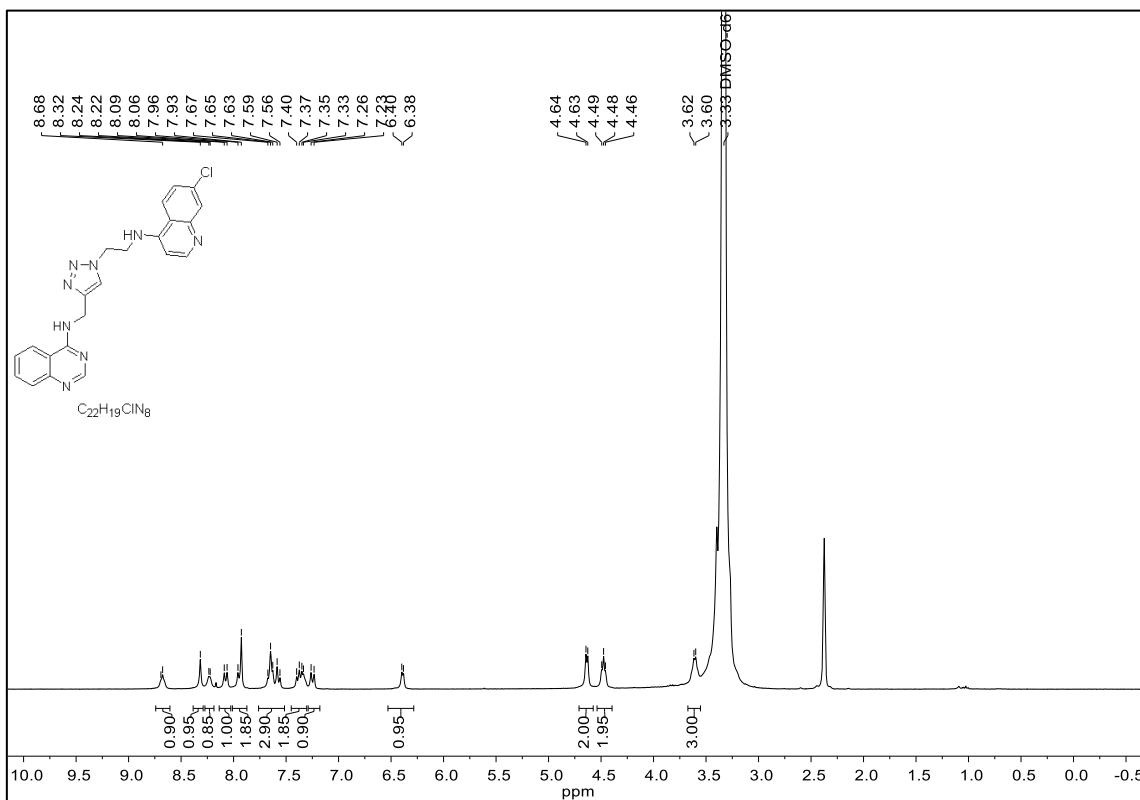
Analysis Name D:\Data\PROF. IVONE\SPM 61_POS.d
Method Tune_Low_Tomaz_Pos_1300u_Willian 1.m
Sample Name SPM 61_POS
Comment

Acquisition Date 11/1/2017 9:34:39 AM

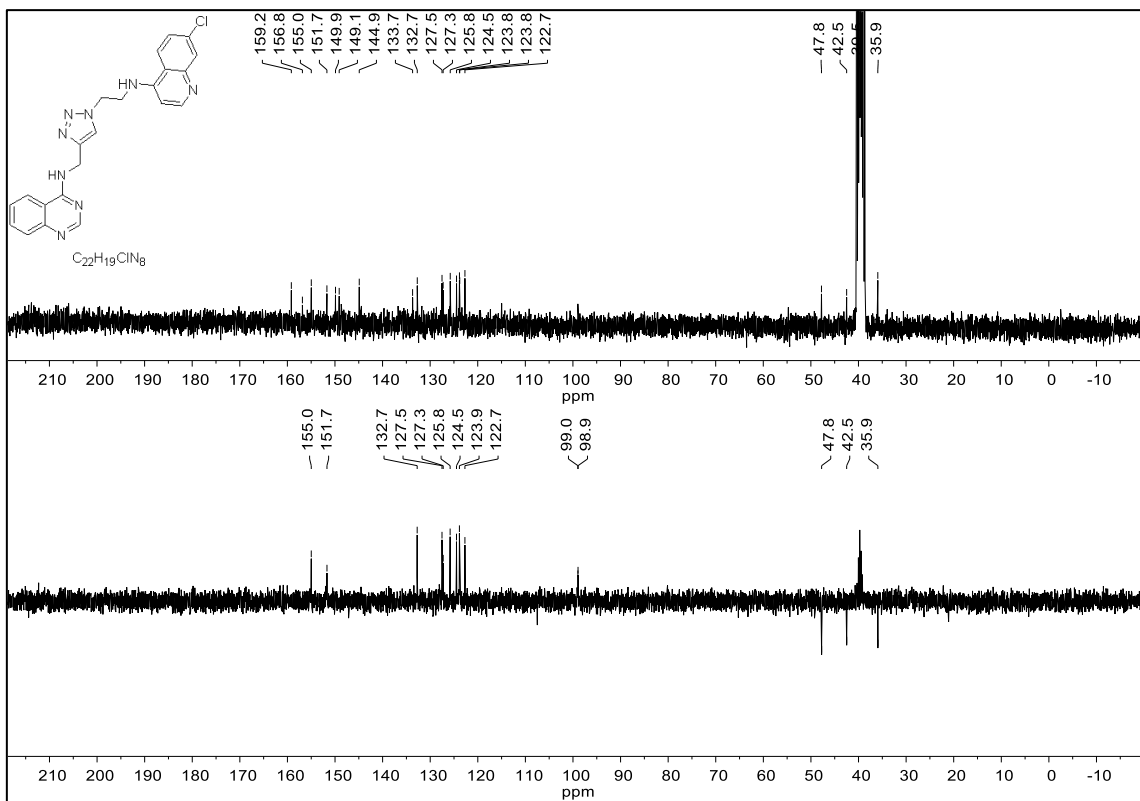
Operator TOMAZ
Instrument micrOTOF-Q



^1H NMR (300 MHz, $\text{DMSO-}d_6$) – Compound **05**



^{13}C NMR (75 MHz, $\text{DMSO-}d_6$) – Compound **05**



HRMS (ES⁺) – Compound 05

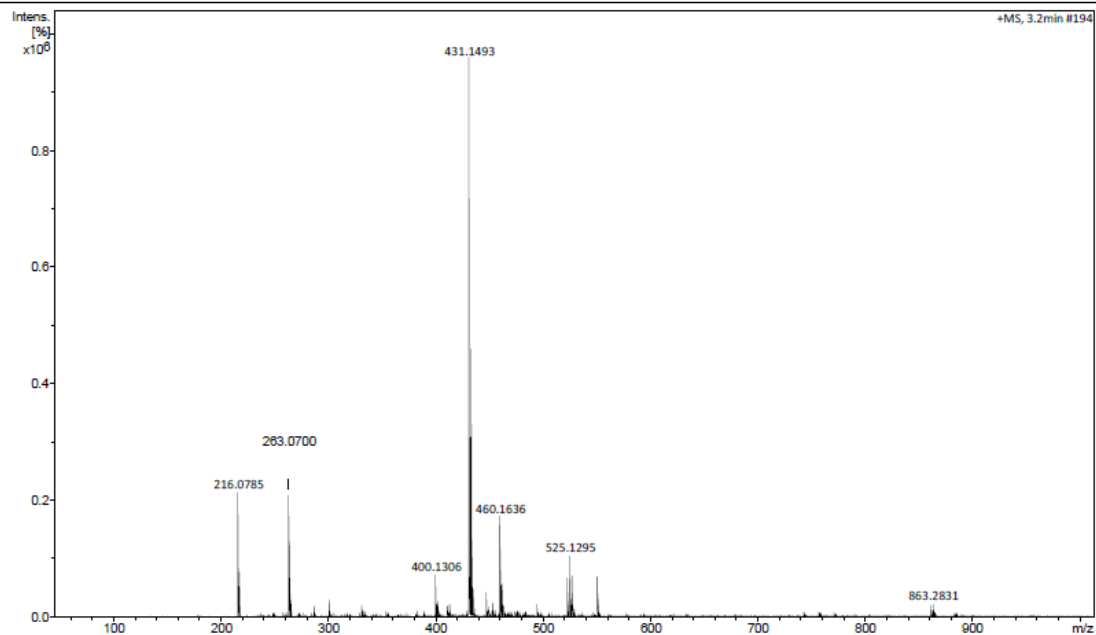
Generic Display Report

Analysis Info

Analysis Name D:\Data\PROF. IVONE\SPM 66_POS.d
 Method Tune_Low_Tomaz_Pos_1300u_Willian 1.m
 Sample Name SPM 66_POS
 Comment

Acquisition Date 11/1/2017 9:58:19 AM

Operator TOMAZ
 Instrument micrOTOF-Q



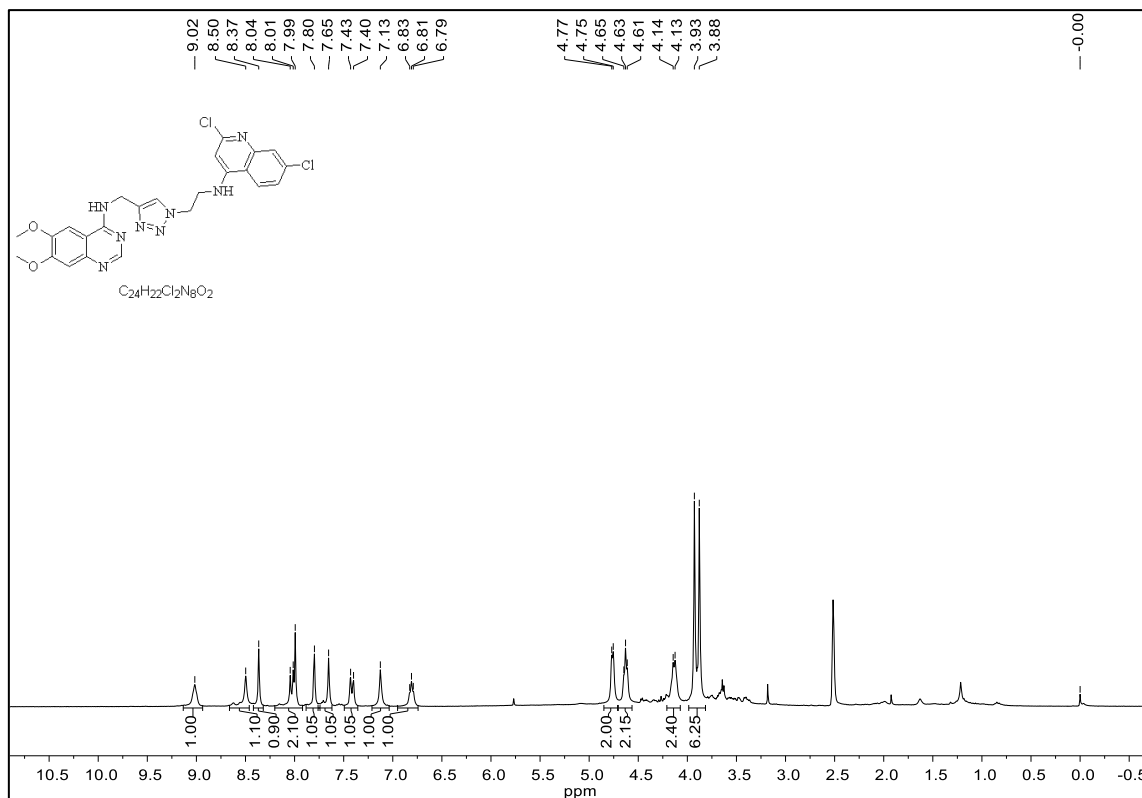
Bruker Compass DataAnalysis 4.3

printed: 11/1/2017 10:08:18 AM

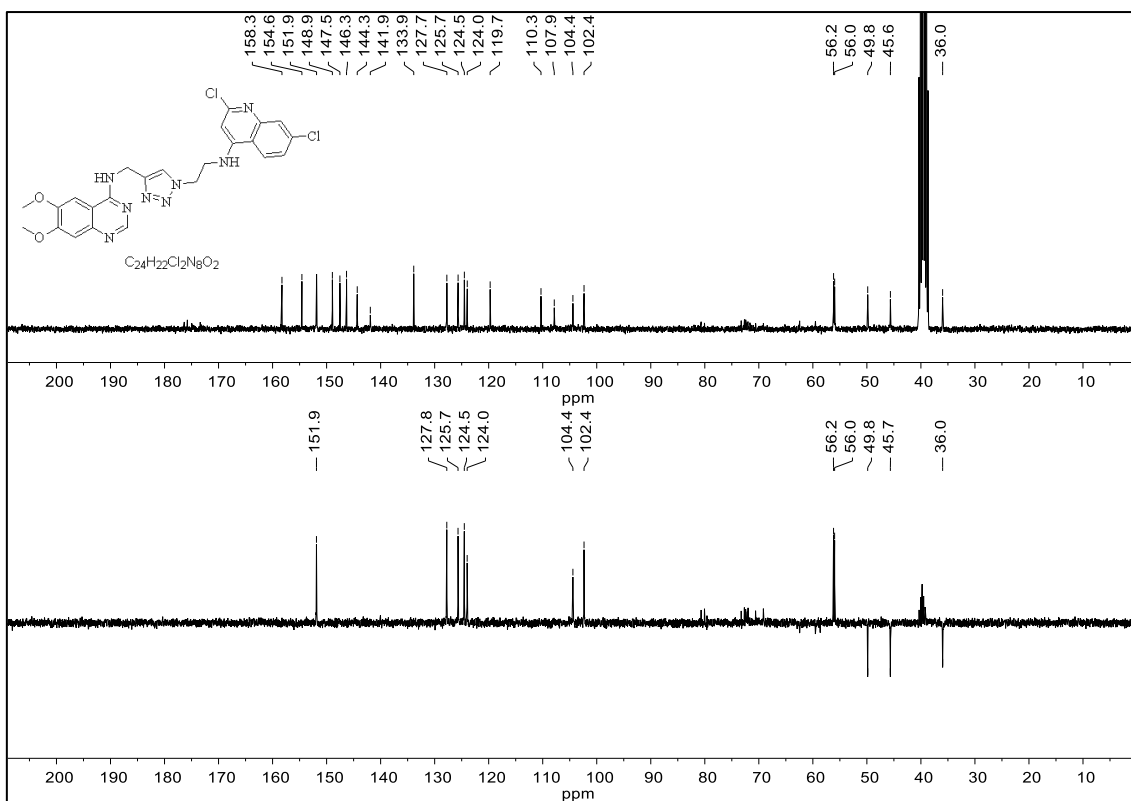
by: TOMAZ

Page 1 of 1

¹H NMR (300 MHz, DMSO_d₆) – Compound 06



¹³C NMR (75 MHz, DMSO-d₆) – Compound 06



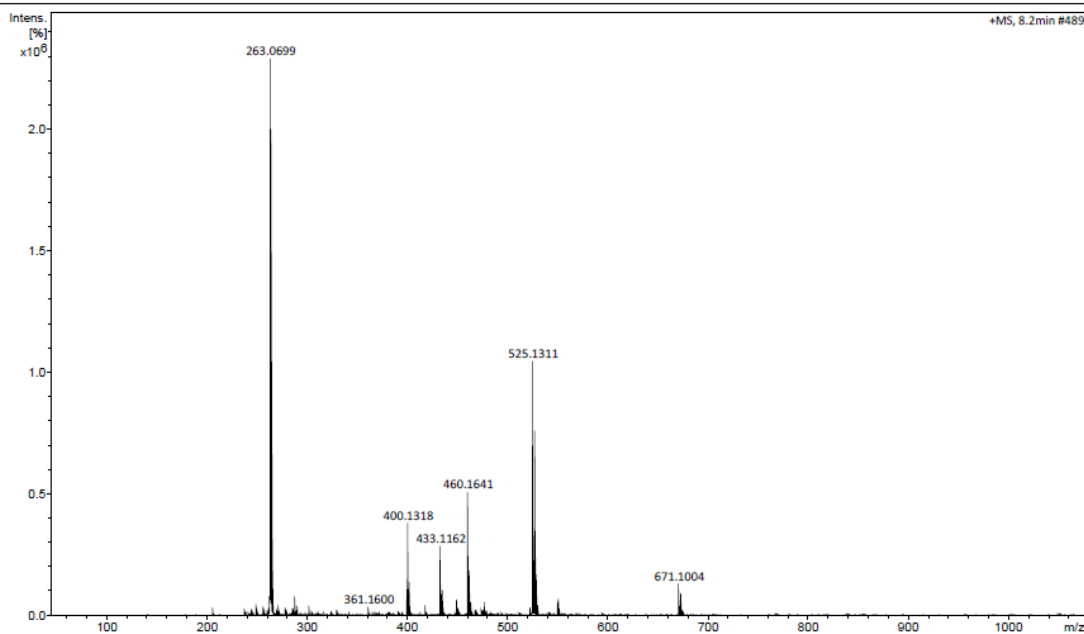
HRMS (ES⁺) – Compound 06

Generic Display Report

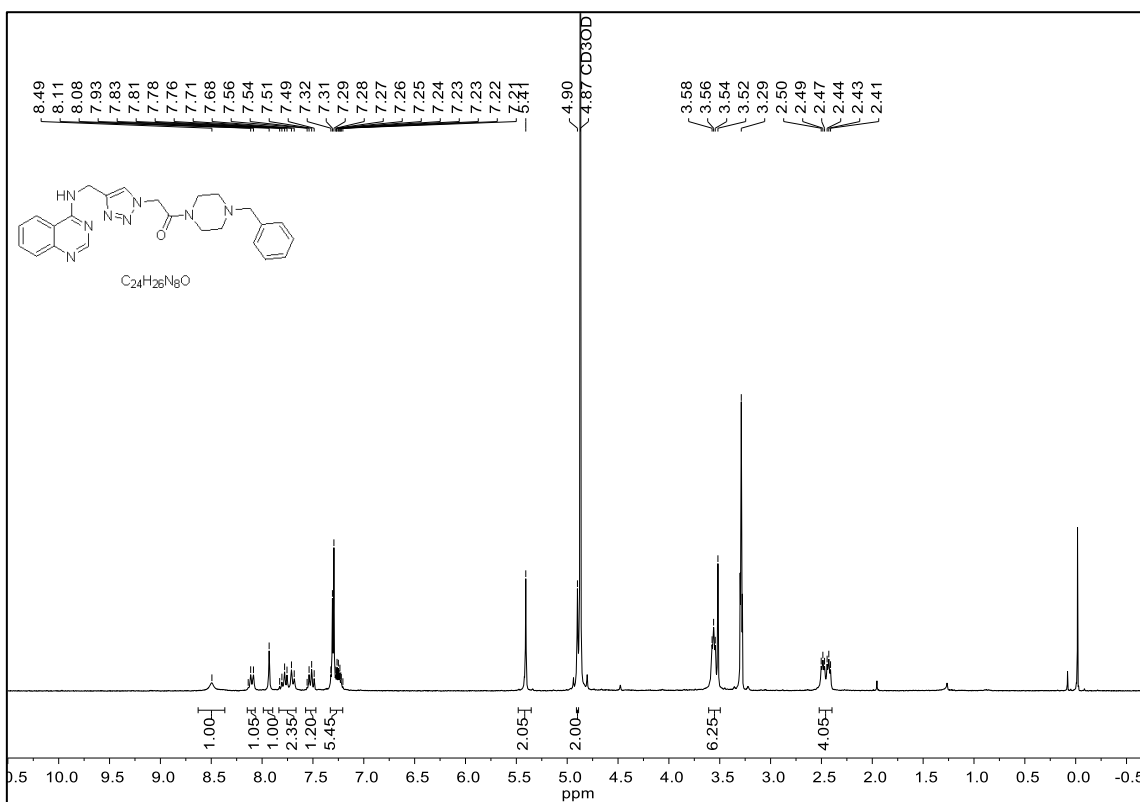
Analysis Info

Analysis Name: D:\Data\PROF. IVONE\SPM 65_POS.d
Method: Tune_Low_Tomaz_Pos_1300u_Willian 1.m
Sample Name: SPM 65_POS
Comment:

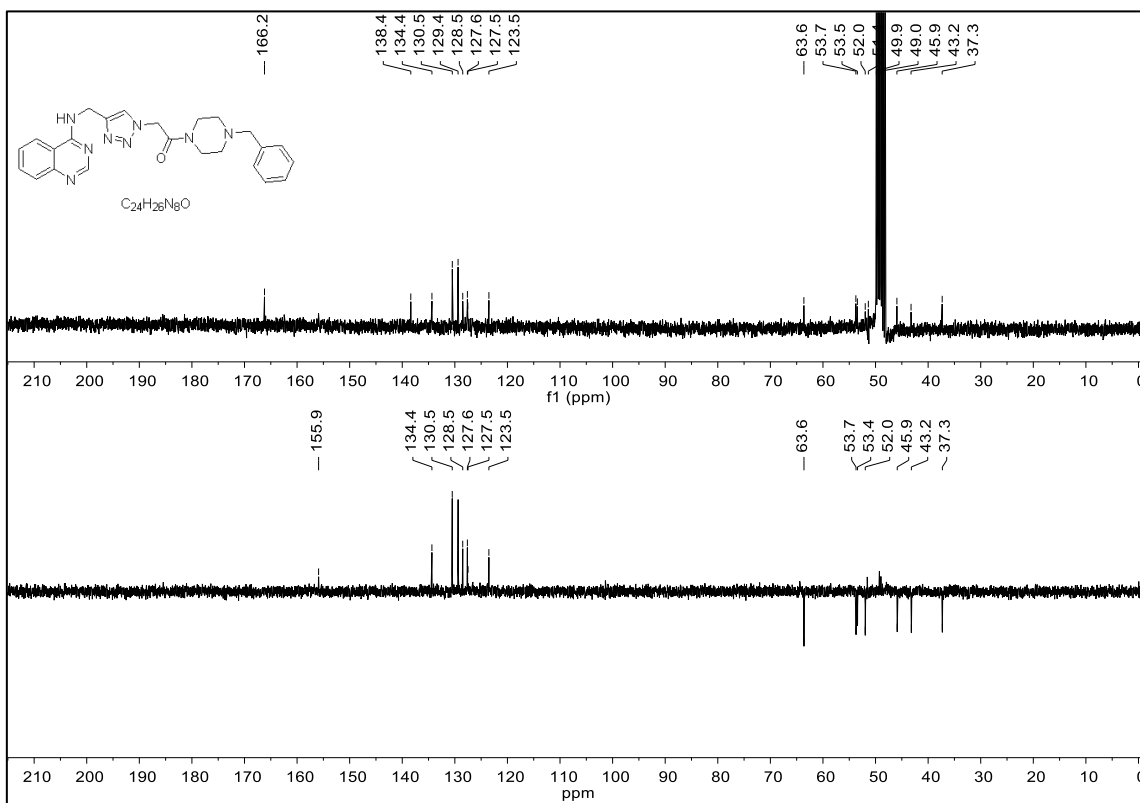
Acquisition Date: 11/1/2017 9:44:20 AM
Operator: TOMAZ
Instrument: micrOTOF-Q



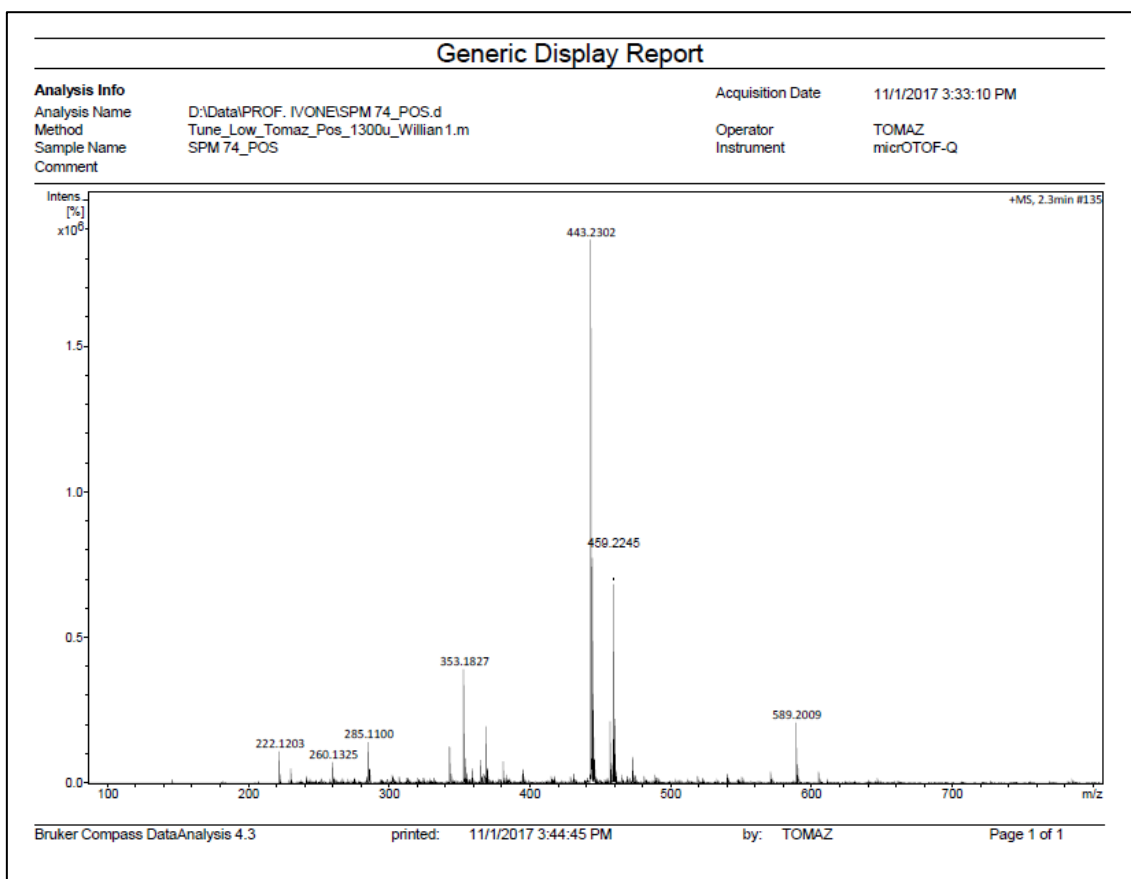
¹H NMR (300 MHz, CD₃OD) – Compound 13



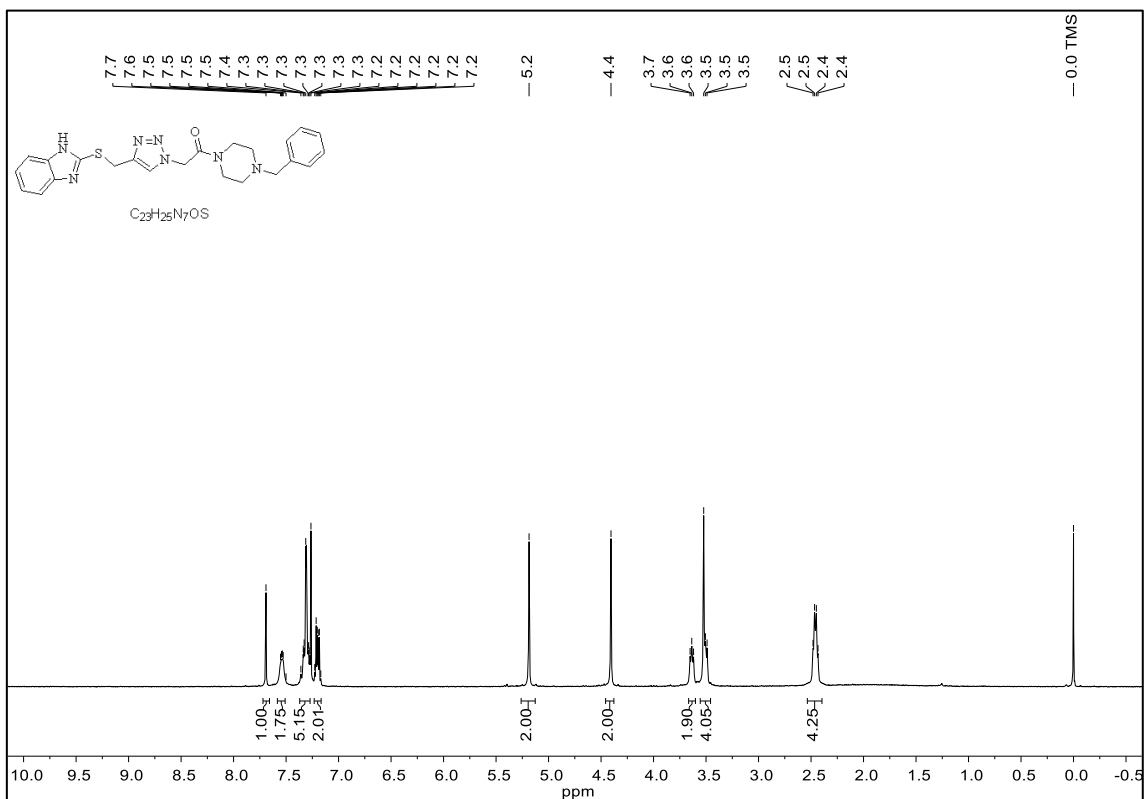
¹³C NMR (75 MHz, CD₃OD) – Compound 13



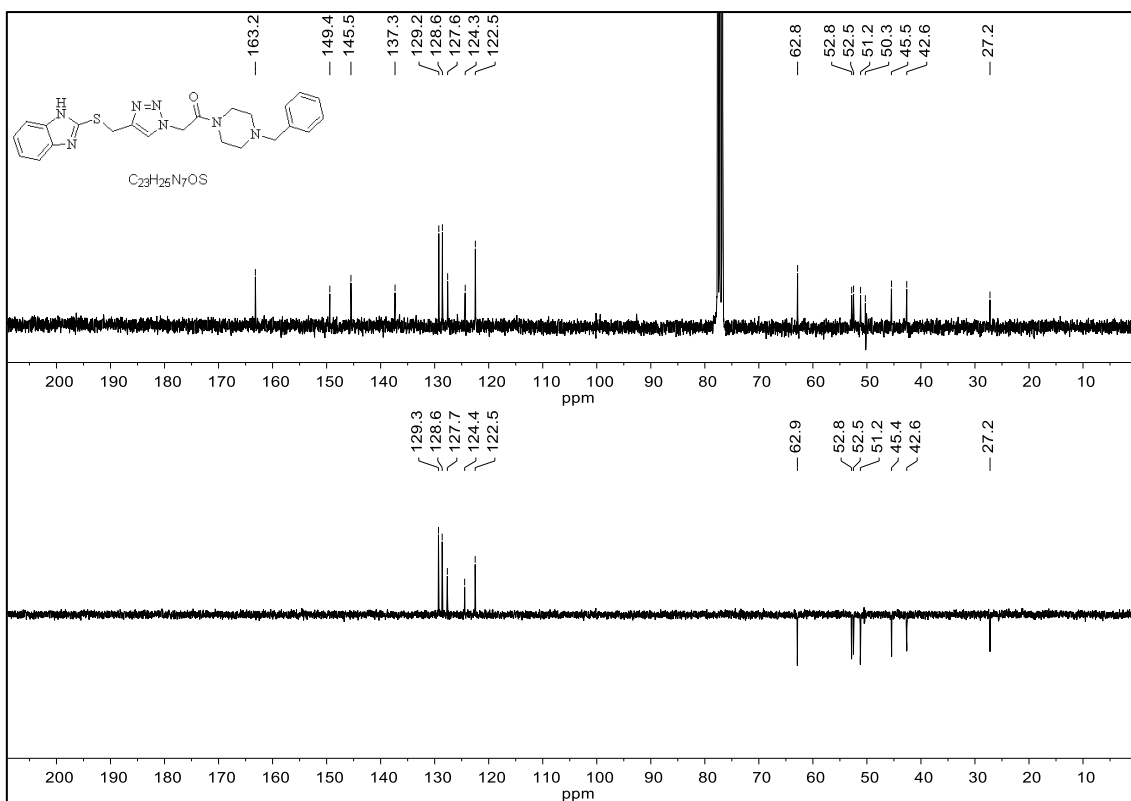
HRMS (ES⁺) – Compound 13



¹H NMR (300 MHz, CDCl₃) – Compound 15



¹³C NMR (75 MHz, CDCl₃) – Compound 15



HRMS (ES⁺) – Compound 15

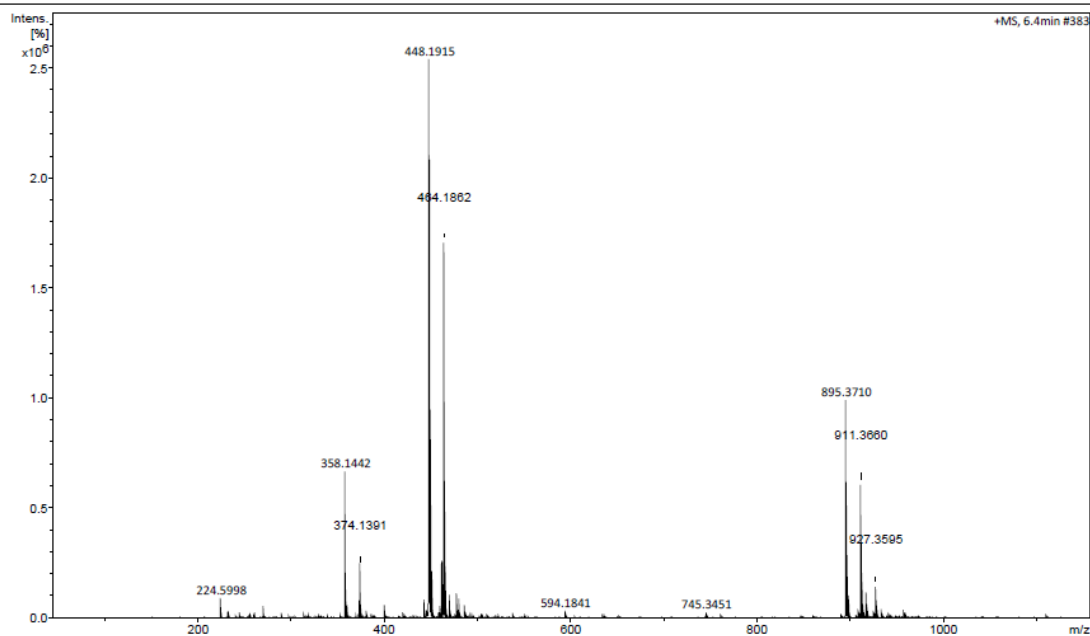
Generic Display Report

Analysis Info

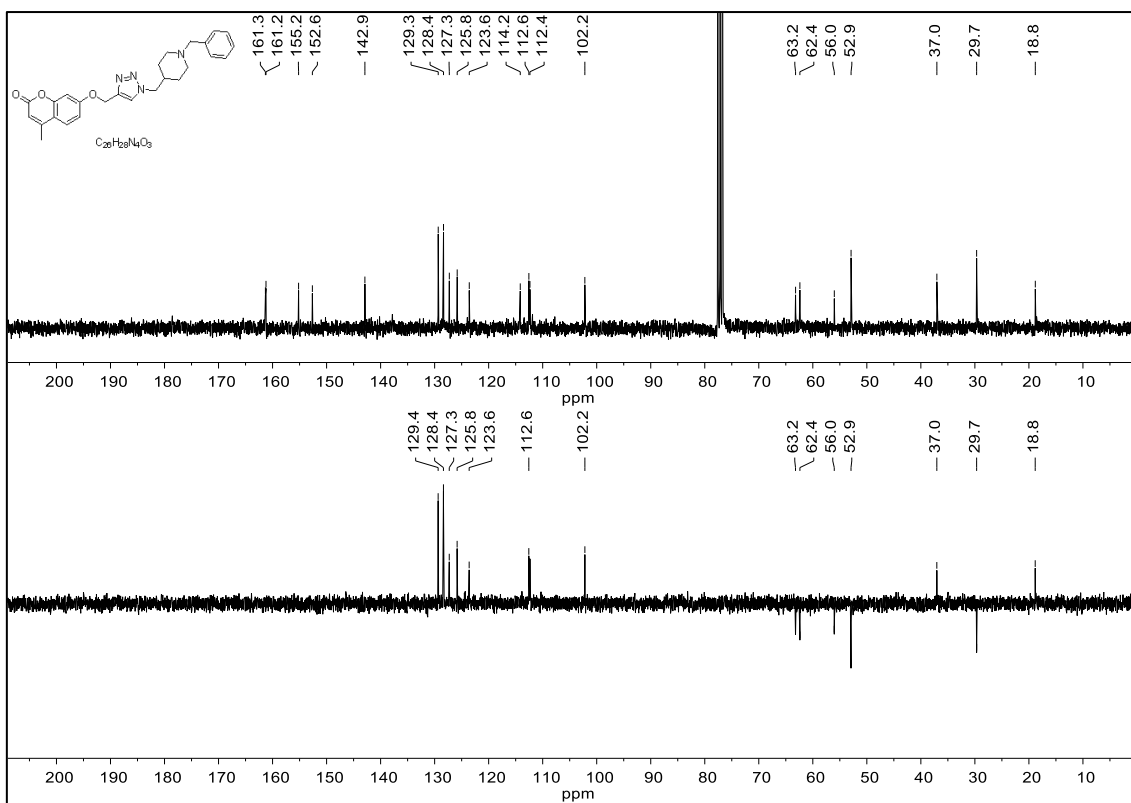
Analysis Name: D:\Data\PROF. IVONE\SPM 75_POS.d
Method: Tune_Low_Tomaz_Pos_1300u_Willian 1.m
Sample Name: SPM 75_POS
Comment:

Acquisition Date: 11/1/2017 3:47:19 PM

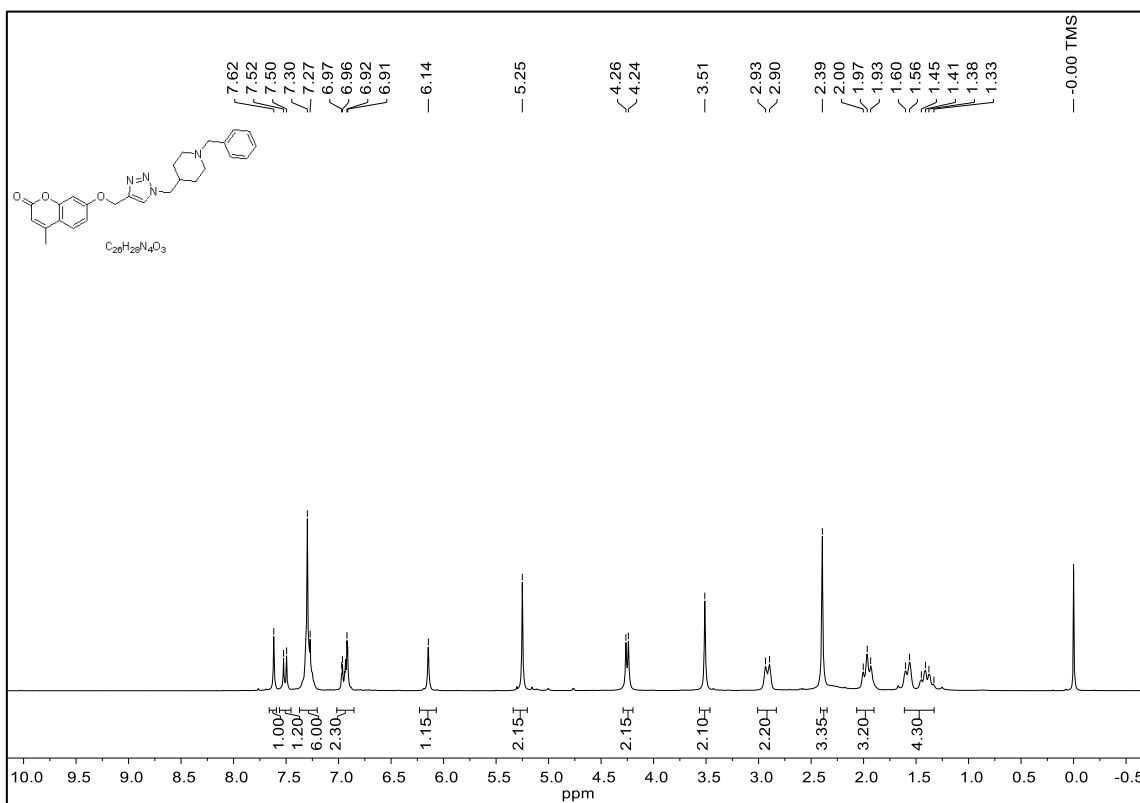
Operator: TOMAZ
Instrument: micrOTOF-Q



^{13}C NMR (75 MHz, CDCl_3) – Compound 25



^{13}C NMR (75 MHz, CDCl_3) – Compound 25



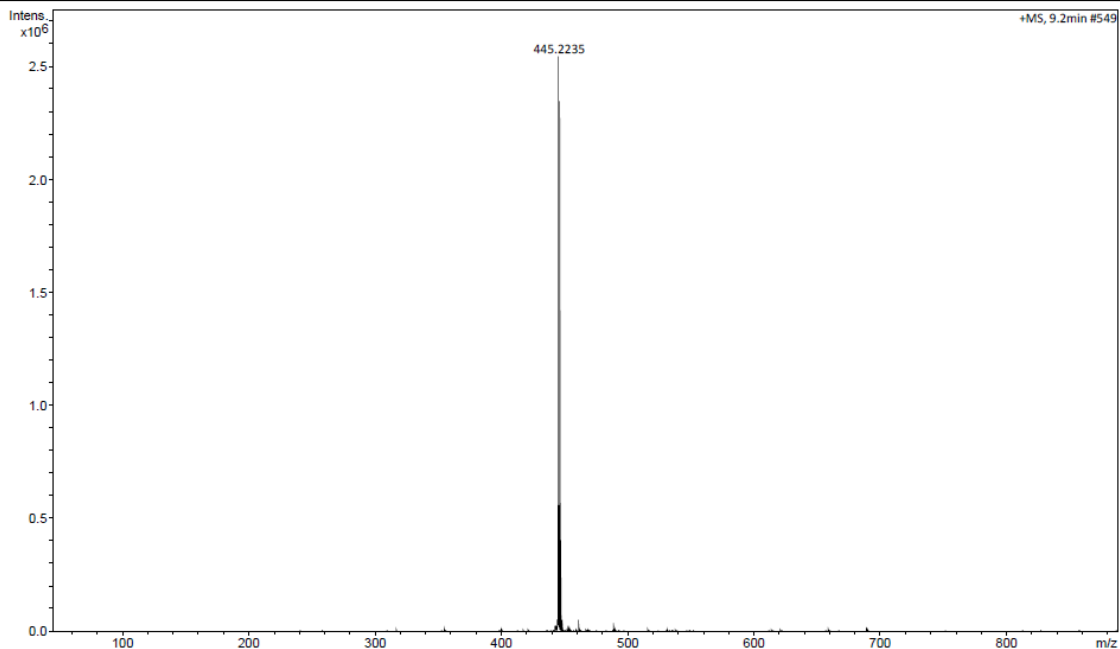
HRMS (ES⁺) – Compound 25

Generic Display Report

Analysis Info

Analysis Name D:\Data\PROF. IVONE\SPM 48_POS.d
Method Tune_Low_Tomaz_Pos_1300u_Willian 1.m
Sample Name SPM 48_POS
Comment

Acquisition Date 11/30/2018 5:06:59 PM
Operator TOMAZ
Instrument micrOTOF-Q



Bruker Compass DataAnalysis 4.3

printed: 12/5/2018 2:25:21 PM

by: TOMAZ

Page 1 of 1

Cell culture

HTLV-1-infected T-cell line MT-2 (88051601, from European Collection of Authenticated Cell Cultures – ECACC) was maintained in Roswell Park Memorial Institute Medium (RPMI-1640, Gibco Life Sciences) supplemented with 10% heat inactivated fetal bovine serum (FBS, Hyclone). Jurkat LTR-GFP cell line was provided by Luc Willems and Renaud Mahieux² for the establishment of an inducible reporter cell line (Jurkat LTR-GFP inducible-*tax*), which was cultured under the same conditions as MT-2. Huh-7 cell line (human hepatoma cell line), kindly provided by Dr. Amilcar Tanuri from Federal University of Rio de Janeiro, was maintained in Dulbecco's Modified Eagle's Medium/Ham's Nutrient Mixture F12 (DMEM F12, Sigma-Aldrich) containing 10% FBS. The culture of all cell lines was kept at 37° C in 5% CO₂ and 85% relative humidity.

Screening of compounds by a cell-based assay using resazurin reduction method in HTLV-1-infected cell line (MT-2)

All compounds were dissolved in dimethyl sulfoxide (DMSO, Sigma-Aldrich) to a final concentration of 10 mM and stored in aliquots at -20° C. Etoposide (ETO, Sigma-Aldrich) was used in this study as a control compound. In order to identify compounds that interfere with cell growth and/or viability, we performed a screening using resazurin reduction method. For this, 3 μ l of the compound from stock solution (10 mM) were transferred to polypropylene 384-well plates (Greiner Bio-One), containing 97 μ l of PBS, yielding a final compound concentration of 0.3 mM in 3% of DMSO (v/v 33.33-fold dilution). To evaluate the compound activity, 10 μ l of compound solution were transferred into tissue culture-treated black polystyrene 384-well assay plates (Greiner Bio-One). Following that, MT-2 cell line (50 μ l of cell suspension/well) was plated jointly with the 25 compounds. Thus, the final compound concentration was 50 μ M in 0.5% DMSO (v/v). MT-2 cell line treated with etoposide (ETO) at 20 μ M and MT-2 with 0.5% DMSO were used as positive and negative controls, respectively. Wells with only culture medium were maintained as control of background fluorescence. Before reaching 72 h of incubation, resazurin (Sigma-Aldrich) at 10 μ M was added to all wells and the microplate was further incubated for 4 h. Then, resazurin reduction (measurement for cell proliferation/metabolic activity) was quantified by fluorescence at 590 nm using SpectraMax M5 (Molecular Devices). The assay was performed on three independent days.

Data normalization

The data for *relative fluorescence units* (RFU) obtained from resazurin assay were normalized to negative (HTLV-1-infected cell line MT-2 with 0.5% DMSO) and positive

(HTLV-1-infected cell line MT-2 with 20 μ M of ETO) controls to establish the normalized activity, according to the equation below:

$$\text{Normalized activity (\%)} = \left(1 - \frac{(\text{Value of RFU MT-2 + compound}) - (\text{Mean of RFU MT-2 + ETO})}{(\text{Mean of RFU MT-2 0.5\% DMSO}) - (\text{Mean of RFU MT-2 + ETO})}\right) * 100$$

Cell cycle analysis

To confirm the activity of selected compounds on HTLV-1-infected cell line (MT-2) proliferation, we evaluated their effects on cell cycle by flow cytometry. In a 24-well plate, 100 μ l/well of compound at 300 μ M and 500 μ l of MT-2 cells (3×10^5 cells/well) were incubated for 72 h at 37° C in 5% CO₂ and 85% relative humidity. Etoposide (ETO) at 20 μ M and MT-2 with 0.5% DMSO were employed as positive and negative controls, respectively. After 72 h, cell suspension of each well was collected, washed twice with phosphate buffered saline (PBS) and fixed with ice cold 70% ethanol. After overnight incubation at -20° C, the samples were centrifuged at 400 x g/5 minutes and treated with RNase A (Qiagen) during 30 minutes at 37° C. Finally, cells were centrifuged at 400 x g/5 minutes and stained with propidium iodide (PI) for analysis by flow cytometry (BD FACSCalibur™). The percentage of cells in G0/G1, S and G2/M phases was assessed through *ModFit LT 5.0* software. The assays were also performed in triplicate.

Assessment of apoptosis by caspase-3/7 and annexin-V/PI staining

Apoptosis was evaluated through two assays: caspase-3/7 activation and annexin-V/PI staining. Firstly, selected compounds (100 μ l/well at 300 μ M) were plated jointly with HTLV-1-infected cell line (MT-2) (500 μ l/well at 3×10^5 cells/well) in a 24-well plate for 72 h at 37° C in 5% CO₂ and 85% relative humidity. MT-2 incubated with ETO at 20 μ M and MT-2 with 0.5% DMSO were used in all assays as positive and negative controls, respectively. After 72 h, cells were incubated with CellEvent™ Caspase-3/7

Green Detection Reagent (Thermo Fisher Scientific) during 45 minutes at room temperature in the dark. Later, a total of 10,000 events was acquired by flow cytometry and the data analysis was performed, in which a gate for live cells was selected according to size (forward scatter channel, FSC) and internal complexity (side scatter channel, SSC) of population. Debris and dead cells in low FSC and high SSC were eliminated by this gate. Thus, we determined the total percentage of positive cells for active caspase-3/7 that were present in gate for live cells. From the same samples, it was performed the annexin-V Cy5/PI (BD Biosciences) staining assay according to the manufacturer's instructions. From the gate for live cells, the percentage of cells in early (Annexin-V⁺/PI⁻) and late apoptosis (Annexin-V⁺/PI⁺) was analyzed by flow cytometry (BD FACSCalibur™, using *FlowJo v10* software). We considered the total percentage of cells positive for annexin-V (early and late apoptosis). These assays were performed in triplicate.

Establishment of a reporter cell line: Jurkat LTR-GFP inducible for tax expression

The viral *tax* gene was cloned into the pLenti CMVtight Blast DEST (w762-1) vector from Addgene (#26434) by Gateway cloning system. The production of lentiviral vectors (2nd generation) and generation of the Jurkat LTR-GFP inducible-*tax* cell line was performed by the GIGA Viral Vectors Platform from University of Liège and it was based on the 3rd generation inducible gene expression system *Tet-On*® (from Clontech). Firstly, the plasmids pLVX-Tet3G and pLenti6 Tight Tax were transfected separately on Lenti-X™ 293T Cell Line (from Clontech-Takara) along with a lentiviral packaging mix. This mix consisted in a packaging construct containing the *gag*, *pol*, *rev* genes (psPAX2), and an Env plasmid expressing the vesicular stomatitis virus envelope glycoprotein G (VSV-G). After transfection, lentiviral supernatants were harvested, pooled and titered by qRT-PCR (Lentiviral Titration Kit LV900 from AbmGood) to be further utilized for transduction. Then, the Jurkat LTR-GFP cell line² (5 x 10⁵ cells/mL) was co-transduced

with lentiviral vectors pLVX-Tet3G at a multiplicity of infection (MOI) of 30, and with pLenti6 Tight Tax at a MOI of 16 (Jurkat LTR-GFP inducible-*tax*). Jurkat LTR-GFP Tet3G control was generated by transduction with only lentiviral vector pLVX-Tet3G. For this transduction step, the reagent protamine sulfate (MP Biomedicals) was used according to the manufacturer's instructions (8 µg/mL). Subsequently, cells were centrifuged at 800 x g for 30 minutes at 37° C. The pellet was suspended in RPMI-1640 containing 10% of FBS and cells were incubated at 37° C in 5% CO₂ and 85% relative humidity. After 72 h, cells were cultivated in cell culture medium containing blasticidin in order to select transduced cells, which were expressing the gene of interest. These cells were maintained in blasticidin until the non-transduced cells died as determined by Trypan Blue staining. In addition, a cell sorting (BD FACSAria III) was performed to select the ones expressing GFP after *tax* induction by doxycycline.

Characterization of Jurkat LTR-GFP inducible-tax reporter cell line

Doxycycline was used to induce *tax* gene expression in Jurkat LTR-GFP inducible-*tax* cell line. In order to determine the minimum doxycycline concentration for our assays in a 24-well plate, cells were incubated with different concentrations (0.01, 0.1 and 1 µg/mL) of doxycycline (Sigma-Aldrich) at 37 °C in 5% CO₂ and 85% relative humidity for 72 h. At the same time, Jurkat LTR-GFP Tet3G (control) was also incubated with different concentrations of doxycycline. Cells without this tetracycline derivative were used as controls. After 72 h, GFP expression was evaluated by fluorescence microscopy (FSX100 Olympus). Tax and GFP expressions were also assessed by flow cytometry (BD FACSCalibur™, using *FlowJo v10* software). Thus, an intracellular staining of Tax was performed using the primary mouse antibody anti-Tax, clone LT-4 (kindly provided by Yuetsu Tanaka from Kitasato University, Kanagawa, Japan). Cells

incubated with isotype antibody and just secondary antibody were also used as controls for staining.

Identification of viral Tax transactivation inhibitors using reporter cell line

The reporter cell line Jurkat LTR-GFP inducible-*tax* was used to evaluate the activity of selected compounds on *tax* expression through the GFP signal. In a 24-well plate, 100 µl/well of compound at 300 µM were incubated with 3×10^5 cells/well (500 µl/well) for 72 h at 37° C in 5% CO₂ and 85% relative humidity. Jurkat LTR-GFP Tet3G control and Jurkat LTR-GFP inducible-*tax* with doxycycline were utilized as negative and positive controls, respectively. After 72 h, the cell suspension of each well was collected and stained with PI for analysis by flow cytometry (BD FACSCalibur™). The percentage of cells GFP⁺ and PI⁻ (viable GFP cells) was assessed using dot plots through *FlowJo v10* software.

Cytotoxicity assay using human hepatoma cell line (Huh-7)

The human hepatoma cell line Huh-7 was chosen for the cytotoxicity assay in order to assess the cellular viability after incubation with active compounds. The compounds selected in previous tests were serially diluted in a 1:2 ratio in PBS 1X (v/v) to yield 10-concentration test points (starting at 50 µM) and 10 µl were transferred into tissue culture-treated black polystyrene 384-well assay plates (Greiner Bio-One). Thereafter, 50 µl/well of Huh-7 cells (3.6×10^4 cells/mL) were added in each well and all plates were incubated at 37° C in 5% CO₂ and 85% relative humidity. Before reaching 72 h incubation, 10 µM resazurin (Sigma-Aldrich) was added to all the wells and the microplate was further incubated for 4h. After resazurin readout, cellular viability of Huh-7 was determined according to the equation below:

$$\text{Cellular viability} = \frac{\text{Value of RFU Huh - 7 + compound}}{\text{Mean of RFU Huh - 7 + 0.5 \% DMSO}}$$

2. Supplementary Figures (S1-S4)

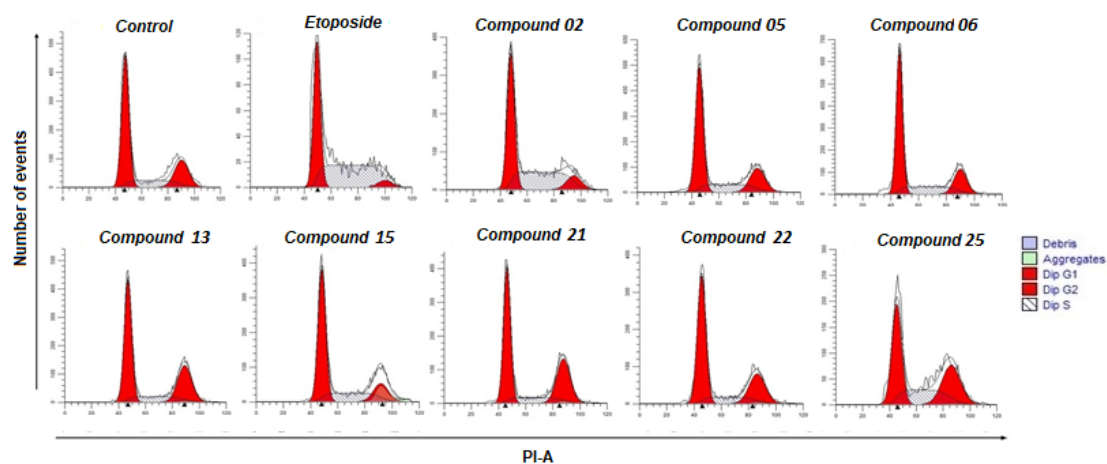


Figure S1. Representative analysis of cell cycle of MT-2 cell line after incubation of 1,2,3-triazole derivatives. It was performed the acquisition of 10,000 events by flow cytometry (BD FACSCalibur™). Cell cycle analysis was obtained through *ModFit LT 5.0* software.

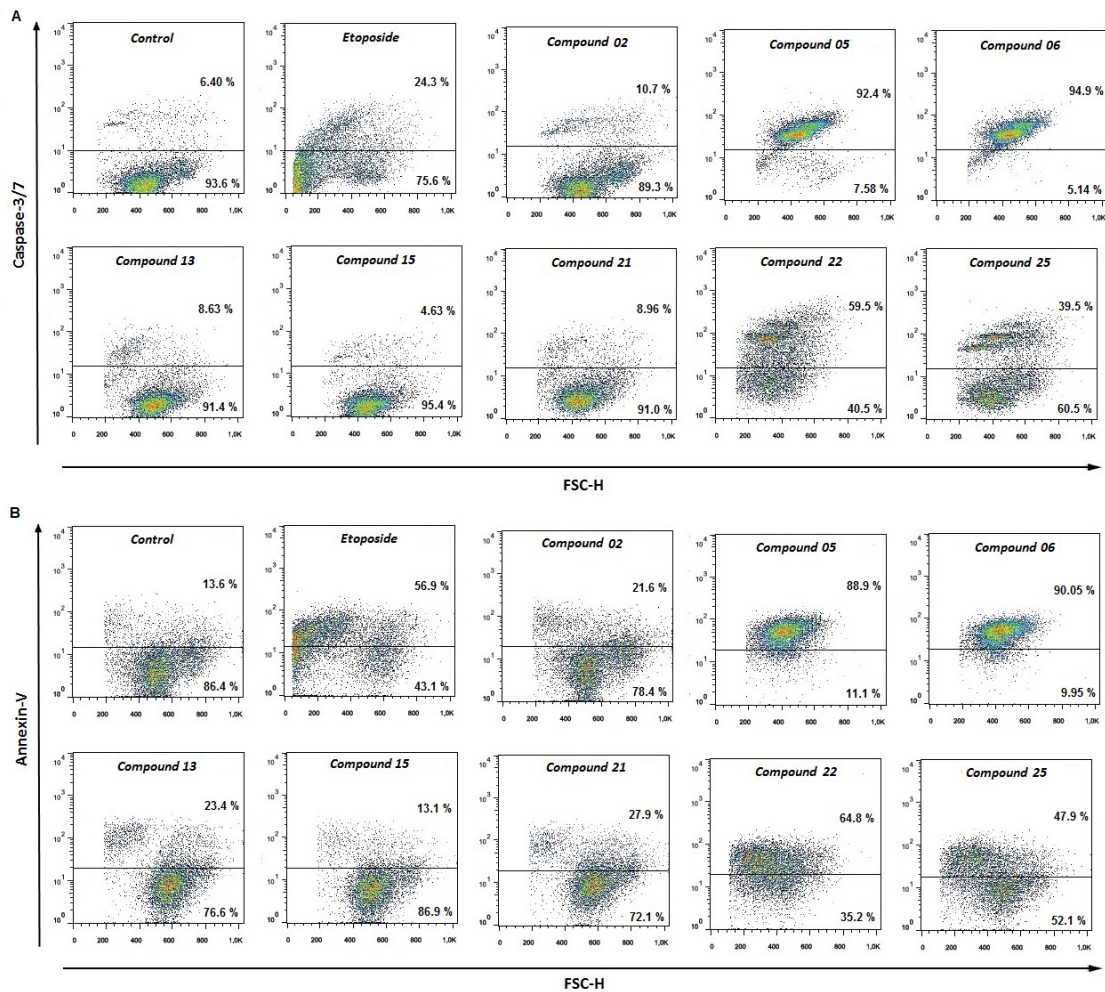


Figure S2. Representative analyses of caspase-3/7 activation and annexin-V staining in MT-2 cell line after incubation with 1,2,3-triazole derivatives. A total of 10,000 events was acquired by flow cytometry (BD FACSCalibur™). For analysis, using *FlowJo v10* software, a gate was performed according to size (forward scatter channel, FSC) and internal complexity (side scatter channel, SSC) of population, following by the determination of percentage of positive cells for caspase-3/7 (A) and annexin-V Cy5 (B), which is represented in each quadrant.

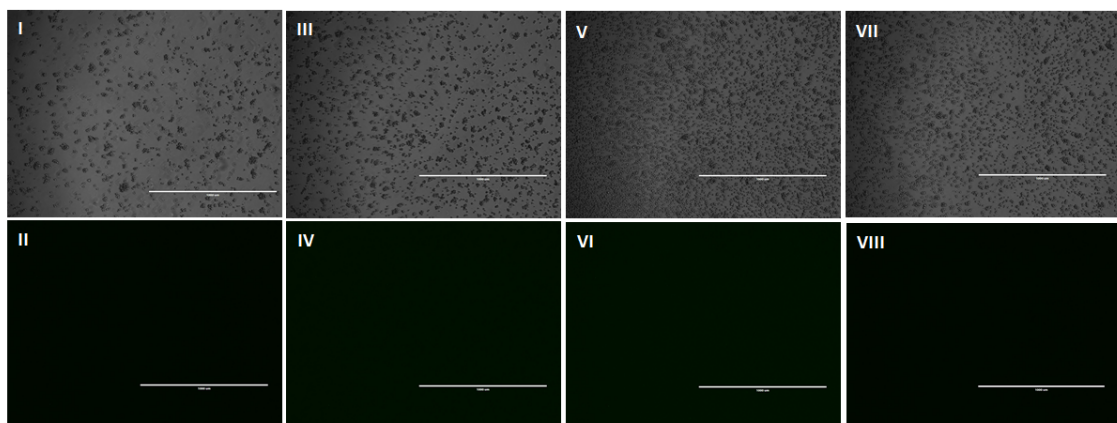


Figure S3. Analysis of GFP expression on Jurkat LTR-GFP Tet3G control cell line after incubation with different concentrations of doxycycline during 72 h. Representative images of cells: I-II) without doxycycline; III-IV) 0.01 $\mu\text{g}/\text{mL}$; V-VI) 0.1 $\mu\text{g}/\text{mL}$; VII-VIII) 1 $\mu\text{g}/\text{mL}$. Magnification: 4X. Scale bar: 1,000 μm .

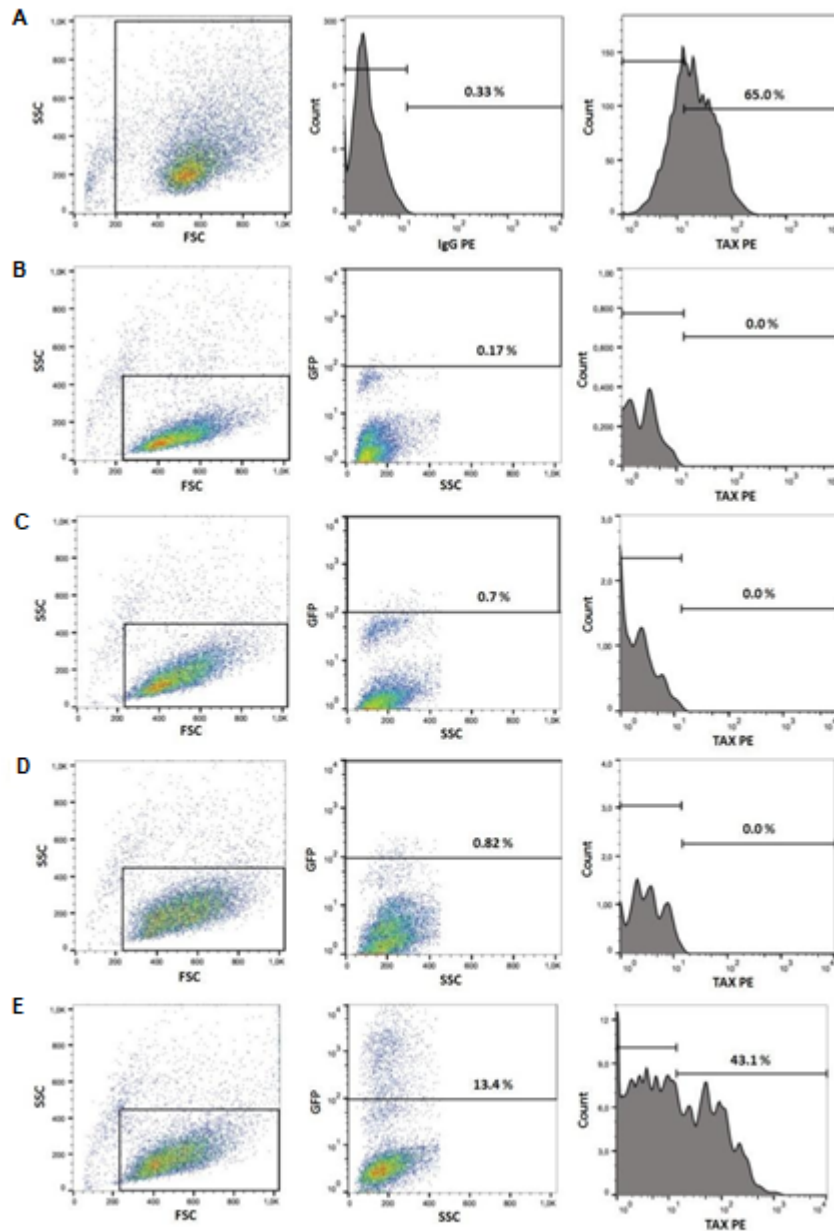


Figure S4. Tax and GFP expression on Jurkat LTR-GFP inducible-*tax* cell line after doxycycline induction for 72 h. A total of 10,000 events was acquired by flow cytometry. For analysis, a gate was performed according to size (forward scatter channel, FSC) and granularity (side scatter channel, SSC), followed by a gate on a positive GFP population. Then, histograms were obtained for Tax expression analysis. A) MT-2 cell line; B) Jurkat LTR-GFP Tet3G control; C) Jurkat LTR-GFP Tet3G control + doxycycline; D) Jurkat LTR-GFP inducible-*tax*; E) Jurkat LTR-GFP inducible-*tax* + doxycycline.

3. References

1. De Andrade P, Mantoani SP, Nunes PSG, et al. Highly potent and selective aryl-1,2,3-triazolyl benzylpiperidine inhibitors toward butyrylcholinesterase in Alzheimer's Disease. *Bioorg Med Chem.* 2019;27:931–943. <https://doi.org/10.1016/j.bmc.2018.12.03026>.
2. Alais S, Mahieux R, Dutartre H. Viral source-independent high susceptibility of dendritic cells to human T-cell leukemia virus type 1 infection compared to that of T lymphocytes. *J Virol.* 2015;89:10580–10590. <https://doi.org/10.1128/JVI.01799-15>.